

**TESTING THE SR/CA PROXY FOR SEA SURFACE
TEMPERATURE RECONSTRUCTION IN THE CORAL
PORITES LUTEA IN GUAM, MICRONESICA**

**BY
AMANDA L. DEVILLERS**

**A thesis submitted in partial fulfillment of the
requirements for the degree of**

**MASTERS OF SCIENCE
IN
BIOLOGY**

**UNIVERSITY OF GUAM
NOVEMBER 2013**

Table of Contents:

Chapter 1: Introduction	1
Chapter 2: Methods	13
<i>Coral Sampling</i>	13
<i>CT Scan and Coral Growth Parameter</i>	15
<i>Metal/Ca Ratio Measurements</i>	16
<i>Sea Surface Temperature and other Environmental Time Series</i>	17
<i>Determination of Chronology</i>	18
<i>Sr/Ca-SST Model Determination and Analysis</i>	19
<i>Analysis of other metals and environmental factors</i>	20
Chapter 3: Results	22
<i>Coral Growth and Calcification</i>	22
<i>Sr/Ca</i>	25
<i>Sea Surface Temperature Model</i>	27
<i>Growth-Dependent Sea Surface Temperature Model</i>	35
<i>Other Metal Ratios</i>	39
<i>Other Environmental Influences</i>	43
<i>Results Summary</i>	53
Chapter 4: Discussion	57
<i>Sr/Ca-SST relationship</i>	57
<i>Growth-dependent Sr/Ca-SST Model</i>	58
<i>Environmental Parameters</i>	63
<i>Other metal/Ca datasets</i>	70

<i>Conclusions and Recommendations</i>	72
References	73
Appendix A: Coral core metadata and colony photographs	80
Appendix B: Sea surface temperature (SST) dataset comparison	91
Appendix C: Raw Sr/Ca datasets	94
Appendix D Empirical Orthogonal Function (EOF) Analysis	98

List of Tables:

Table 3.1. Descriptive statistics for monthly skeletal density values 1985-2010.....	22
Table 3.2 Descriptive statistics for raw Sr/Ca measurements, Sr/Ca values after processing, and Sr/Ca values from Bell <i>et al.</i> 2011a.....	26
Table 3.3 Regression coefficients (R^2) for Sr/Ca and SST for all months, dry months (Dec-Mar), wet months (Jun-Sep), annual averages and wet and dry season averages. ...	33
Table 3.4 Simple regression results for monthly Sr/Ca and skeletal density 1985-2010 .	35
Table 3.5 Simple regression results for monthly skeletal density and SST 1985-2010 ...	35
Table 3.6 Multiple regression results for monthly Sr/Ca, SST and skeletal density 1985-2010	36
Table 3.7 Simple regression results for annual skeletal density, Sr/Ca and SST 1985-2010	37
Table 3.8 Simple regression results for annual linear extension rate, Sr/Ca and SST 1985-2010	37
Table 3.9 Simple regression results for annual calcification rate, Sr/Ca and SST 1985-2010	37
Table 3.10 Multiple regression results for annual Sr/Ca, skeletal density and SST 1985-2010.	38
Table 3.11 Multiple regression results for annual Sr/Ca, linear extension rate and SST 1985-2010	38
Table 3.12 Multiple regression results for annual Sr/Ca, calcification and SST 1985-2010	39
Table 3.13 Correlation coefficients (R) for monthly metal/Ca ratios and Sr/Ca.....	40

Table 3.14 Simple regression results for monthly metal/Ca ratios, SST and skeletal density 1985-2010.	41
Table 3.15 Regression coefficients (R^2) for annual metal/Ca ratios, SST, skeletal density, linear extension rate, and calcification.	42
Table 3.16 Multiple regression results for U/Ca (Monthly and Annual), SST and skeletal density 1985-2010.	43
Table 3.17 Correlation coefficients between SST and the other environmental parameters	46
Table 3.18 Simple regression results between monthly Sr/Ca and environmental parameters 1985-2010	47
Table 3.19 Stepwise regression results for monthly Sr/Ca vs. six environmental parameters (SST, rainfall, MEI, wave height, mean sea level, average period)	48
Table 3.20 Simple regression results between annual Sr/Ca and environmental parameters 1985-2010	49
Table 3.21 Simple regression results between monthly skeletal density and environmental parameters 1985-2010	50
Table 3.22 Stepwise regression results between monthly density and environmental parameters 1985-2010	51
Table 3.23 Simple regression results between annual density and environmental parameters 1985-2010	52
Table 3.24 Stepwise regression results between annual skeletal density and environmental parameters 1985-2010	52
Table 3.25 Summary of Sr/Ca regression results.	54
Table 3.26 Summary of coral growth regression results.....	55

Table 3.27 Summary of U/Ca regression results.	56
Table A-1 Coral colony coordinates and diver information.....	80
Table A-2 Coral colony dimensions.	80
Table B-1 Descriptive statistics for the Asan and Agat reef flat HOBO loggers and the CDIP Wave Buoy off of Ipan for hourly measurements taken between September 28, 2012 and December 17, 2012.....	92
Table D-1 Percent of total variance explained by each EOF mode.....	98
Table D-2 Normalized Eigenmodes for each EOF mode and each metal/Ca ratio.	98
Table D-3 Percent of variance of each metal/Ca ratio explained by each EOF mode	99

List of Figures:

Figure 1.1 Relationship model between SST, Sr/Ca, and coral growth	12
Figure 2.1 Maps of coring sites	14
Figure 3.1 Annual skeletal density measurements 1985-2010.....	23
Figure 3.2 Annual linear extension rates 1985-2010.....	24
Figure 3.3 Annual calcification rates 1985-2010	24
Figure 3.4 Annual Sr/Ca measurements 1985-2010.....	26
Figure 3.5 Apra2-1 Sr/Ca-SST analysis.....	28
Figure 3.6 Agat1-1 Sr/Ca-SST analysis.....	29
Figure 3.7 Asan1-1 Sr/Ca-SST analysis.	30
Figure 3.8 Asan2-1 Sr/Ca-SST analysis.	31
Figure 3.9 Regression plots for annual Sr/Ca and SST 1989-1994 for Apra2-1 and Asan1-1	32
Figure 3.10 Sr/Ca-SST calibration equations for Asan1-1 and Asan2-1 monthly datasets compared with the average Porites equation presented by Correge (2006) and that from Bell et al. (2011a).	34
Figure 3.11 Environmental time series for SST, total rainfall, and MEI 1985-2010.....	44
Figure 3.12 Environmental time series for mean sea level, wave height and average period 1985-2010	45
Figure A-1 Whole colony view of Agat1 in April 2012, prior to coring.....	81
Figure A-2 Whole colony view of Agat1 in April 2012, during coring	82
Figure A-3 Whole colony view of Agat1 in March 2013, one year after coring	83
Figure A-4 Whole colony view of Agat2 in April 2012, prior to coring.....	84

Figure A-5 Whole colony view of Agat2 in March 2012, one year after coring	85
Figure A-6 Whole colony view of Asan1 April 2012, prior to coring	86
Figure A-7 Whole colony view of Asan2 April 2012, during coring.....	87
Figure A-8 Whole colony view of Apra1 in April 2012, prior to coring	88
Figure A-9 Whole colony view of Apra1 in November 2012, after coring.....	89
Figure A-10 Whole colony view of Apra2 in November 2012, after coring.....	90
Figure B-1 SST from reef flat HOBO loggers in Asan and Agat compared with SST from the CDIP Wave Buoy in off of Ipan from September 28, 2012 to December 17, 2012.	92
Figure B-2 SST data from Hadley 13-14 degrees N, 144-145 degrees E compared with SST from the CDIP wave buoy off of Ipan, Guam for the time period July 2003 to March 2013. Both datasets are averaged to monthly values.....	93
Figure C-1 Raw Sr/Ca values from Apra2-1 as measured at distances from the top of the core (most recent skeletal material) to the bottom (oldest skeletal material).	94
Figure C-2 Raw Sr/Ca values from Agat1-1 for the first 70 cm of each transect as measured at distances from the top of the core (most recent skeletal material) to the bottom (oldest skeletal material). A and B indicate two separate transects along which Sr/Ca was measured as replicates.....	95
Figure C-3 Raw Sr/Ca values from Asan1-1 for the first 70 cm of each transect as measured at distances from the top of the core (most recent skeletal material) to the bottom (oldest skeletal material).	96
Figure C-4 Raw Sr/Ca values from Asan2-1 as measured at distances from the top of the core (most recent skeletal material) to the bottom (oldest skeletal material).	97

Chapter 1: Introduction

Over the history of the Earth, environmental conditions have been anything but stable. Average global temperatures have fluctuated between ice ages and intermediate warm periods, the sea level has been hundreds of feet above and below the present level, and land masses have been moved, formed and destroyed (Turekian 1996). These changes have occurred over hundreds to millions of years, while instrumental climate records only exist for the past several decades in most locations (Fairbanks et al. 1997). Therefore, information on past climate relies upon preserved climate records in ice cores, fossils, rocks, sediment, and various other media that predate human records (Gagan et al. 2000).

Corals have been an important source of past environmental information. Corals grow continuously, incorporating elements and compounds from the seawater which surrounds them into their stony calcium carbonate skeletons (Lough et al. 1997). They form annual growth rings similar to those found in trees which result from seasonal variation in growth. These rings can be used to accurately date points in the skeleton (Barnes and Lough 1993). Furthermore, corals grow fast enough (generally 5-20 mm/year) to allow sub-annual sampling (Lough et al. 1997). These characteristics have been utilized to obtain information on the climate history from both living and fossil corals. By measuring elemental ratios such as Ba/Ca, Sr/Ca, and Fe/Ca as well as elemental isotopes like $\delta^{18}\text{O}$ and C^{14} from within coral skeletons, coral are used as proxies for the environmental conditions from sea surface temperature and salinity to sediment input and heavy metals pollution (Quinn and Sampson 2002; Fairbanks et al. 1997). Living corals are used to examine the last one or two centuries of environmental

history, while fossil corals have been used to reconstruct certain parameters back to 1,100 years ago (Cobb et al. 2003).

Today, there is global concern regarding anthropogenic-induced acceleration of climate change. In light of this, coral records are even more valuable as coral reefs are one of the most vulnerable communities to climate change impacts (Parmesan 2006). By examining cores collected from living corals, we can gain information not only of past climatic conditions, but also information on how the living reefs are currently coping with changing conditions (Lough et al. 1997).

Guam is a prime location with which to study global climate change. It is located in the Western Pacific Warm Pool; an area greatly affected by El Nino/Southern Oscillation (ENSO) weather patterns. Guam is part of Micronesia, but has longer and more consistent climate records than the other islands, making it a good starting location for reconstructing past climate for the region. Climate records are available from sources such as the United States Air Force and the National Weather Service on Guam since the 1950s (Lander and Guard 2003; Bell et al. 2011a). From these records, some changes to Guam's climate are already discernible. Average air temperature on Guam has been on a general upward trend for the past several decades. Additionally, the sea level has risen significantly (on average 9.4 +/- 6.2 mm per year since 1990). This far exceeds the global average sea level rise and is the result of an increase of wind forcing in the region (Merrifield 2011). Sea surface temperature around Guam has also trended upward over the last half century (Asami et al. 2005; Bell et al. 2011a). Coral biologists have noted bleaching events associated with extreme warm sea surface temperature events which may have increased in frequency in recent years (Burdick et al. 2008), including a major

bleaching event in the summer and early fall of 2013 (Laurie Raymundo, University of Guam Marine Laboratory, personal communication).

A half a century of information, however, is too little to say much about an island's environmental history. It is particularly difficult to gain much information on phenomena such as ENSO events which occur in frequencies most appropriately studied on a decadal scale rather than an annual scale (Asami et al. 2005). Furthermore, available information is limited to the specific sites where data were recorded and are sometimes not an accurate record. Fortunately, Guam is endowed with both living and fossil corals reefs as well as limestone caves, which house speleothems (calcite structures formed by cave drip water that have been studied to reconstruct climate elements; Bell et al. 2011a). These tools can be used to enhance our understanding of the human-recorded environmental history of Guam and reconstruct the environmental history that pre-dates our current records. Here, I will explore just one of these tools, living coral and their ability to record sea surface temperatures (SST).

Numerous proxies for SST have been utilized in the living coral record (Quinn and Sampson 2002). By far, the two most widely applied are the quantity of $\delta^{18}\text{O}$ and the ratio of strontium to calcium ions (Sr/Ca) in the coral skeleton. Sr/Ca is considered the stronger proxy because $\delta^{18}\text{O}$ is affected by both SST and salinity. This is particularly important in areas influenced by low salinity river plumes (McCulloch et al. 1994), which describes the reefs in most of Central and Southern Guam. For this reason, I will focus only on Sr/Ca in the present study.

Sr/Ca is considered a well-established paleontological proxy for SST (Correge 2006). Strontium (Sr^{2+}) and calcium (Ca^{2+}) ions are incorporated into the aragonite

skeleton of scleractinian coral as it builds. The amount of strontium in the seawater is assumed to be constant, although there is in fact minute variability (deVilliers 1999). Strontium incorporation into aragonite (both inorganically and biogenically deposited) is a function of SST and is typically described by Sr/Ca, which decreases linearly as temperature increases (Weber 1973). As mentioned above, annual growth rings are visible in many coral species. Thus, by measuring Sr/Ca at particular locations in the skeleton, we can calculate the SST at a particular point in time by inputting the Sr/Ca value into a model formula.

The model is built by measuring Sr/Ca in corals during times when the SST is known, and using regression analyses (typically Least Squares) to calculate an equation which best estimates the linear relationship (Correge 2006). For example, an early paper on the topic reported that the Sr/Ca-SST relationship from a variety of coral species could be described by the average equation $K = 11.32 - 0.082 * T$ with a coefficient of determination (R^2) of 0.60, where K is $Sr/Ca * 10^3$ and T is SST in degrees Celsius (Smith et al. 1979). Greater R^2 values, up to 0.77, were obtained when focusing on just one species. With the model equation, one can extrapolate back for Sr/Ca records which pre-date instrumental SST records.

Despite the promise that the work of Smith and others showed in the 70s, more accurate laboratory techniques are needed to remove some of the “noise” in the regression analyses (Smith et al. 1979; Houck and Buddemeier 1977). As a result of the acknowledgement of this “noise,” which prevented precise SST reconstruction, there is a gap in Sr/Ca publications in the 80s. Then, in the mid-1990s Sr/Ca research picked up again with promise of more accurate Sr/Ca measurements using thermal ionization mass

spectrometry (Beck et al. 1992). This technique improved the accuracy of the proxy from $\pm 3^{\circ}\text{C}$ to $\pm 0.05^{\circ}\text{C}$, adding significantly to its applicability. The earliest papers which had been published on mass collections of data from across the world (Weber 1973, Smith et al. 1979) were quickly supplemented by numerous papers from the lower latitudes where seasonal variation in SST is only a few degrees (Fairbanks et al. 1997; Lough and Barnes 1997; McCulloch et al. 1994).

To date, Sr/Ca-based SST reconstructions have been made with at least 12 genera. The great majority of studies (more than 40 studies) have focused on massive *Porites* (Correge 2006). Most studies have been in the Pacific Ocean, specifically New Caledonia and the Great Barrier Reef (Stephans et al. 2004; Quinn and Sampson 2002; Gagan et al. 2000; Guilderson and Schrag 1998; McCulloch et al. 1994), but a few have included Caribbean corals as well (Goodkin et al. 2007; Correge 2006). Sr/Ca studies have reflected the increase in SST seen in instrumental records and have been used to identify ENSO signals and other large-scale weather phenomena (Asami et al. 2005; Charles et al. 1997; McCulloch et al. 1994). An excellent review of Sr/Ca findings is found in Correge (2006).

Despite the wide use of the Sr/Ca proxy in paleontology and climatology studies, there is a wealth of scientific controversy over its legitimacy. When the relationship between Sr/Ca in coral skeletons and SST was first confirmed by Weber (1973), he recognized potential complications when using a biological host for such a proxy and found evidence that a coral's growth rate affects Sr/Ca. Since then, many scientist have argued both sides, finding empirical evidence that the proxy is either significantly affected by growth rate (Cohen and Hart 2004; Reynaud et al. 2004; Ferrier-Pages et al.

2002), completely unaffected by growth rate (Gagan et al 1998; Alibert and McCulloch 1997; Smith et al. 1979), or something in between (Allison and Finch 2004).

The proxy is further complicated because the relationship between Sr/Ca and SST appears to vary within both genus and species. Weber (1973) was also the first to recognize this. He analyzed 2,020 coral specimens from 67 genera across 17 localities and found that Sr/Ca in *Acropora* species tended to be high relative to other genera from the same locality. Additionally, linear regression slopes calculated for Sr/Ca and SST were similarly negative, but variable by species (Weber 1973). Few other studies have compared across genera in a single study, but a meta-analysis by Correge (2006) showed that even with the improved precision in ion measurements, recent Sr/Ca-SST calibration equations supported Weber's conclusions. Correge (2006) also demonstrated that there is high degree of variation in calculated calibration equations even within one genus. When entering the value 9.035 mmol Sr/mol Ca (the value associated with 25 degrees Celsius in the mean equation) into an assortment of the published calibration equations for *Porites* species, predicted values of 19 to 32 degrees Celsius were returned.

These inconsistencies between and within genera probably result from several factors. Inconsistent sampling and chemical analysis techniques, the use of different SST datasets, and differing statistical analyses are certainly contributing factors (Correge 2006). However, these variations may point toward biological mechanisms which could affect Sr/Ca incorporation. The Sr/Ca-SST proxy has a living host, so it seems more than likely that the proxy may be influenced by factors other than temperature including, but certainly not limited to, coral growth parameters. The situation has the potential to become confounded as one of the main factors affecting coral growth is temperature

(Weber et al. 1975). Coral growth is also known to be affected by other factors such as light intensity and water quality (Barnes and Lough 1993). Logically, if coral growth is a factor in determining Sr/Ca, then the other factors which affect growth will cause variation in Sr/Ca beyond the effect of temperature.

These inconsistencies revealed in the literature stress the need for caution in the use of Sr/Ca as a proxy for SST. However, all the studies mentioned have found a strong linear relationship between Sr/Ca and SST across decades, and as a result, there is clear value in attempts to improve the proxy. It is unrealistic to think that any proxy is perfect; all climate proxies have some degree of bias (Lough et al. 1997), but without a better understanding of the biological mechanisms behind the Sr/Ca proxy, it cannot be used with confidence.

A growing field of literature is beginning to close the gap of understanding. By examining the biological mechanisms behind the incorporation of Sr^{2+} into the coral skeleton more closely through laboratory experiments, scientists have covered much ground. Reynaud et al. (2004) found Sr^{2+} incorporation in *Acropora verweyi* was positively related to both light and temperature independently in a four-week tank experiment. Furthermore, Sr^{2+} incorporation was highly correlated with Ca^{2+} incorporation. A similar relationship between Sr^{2+} and Ca^{2+} incorporation was identified in an experiment with *Stylophora pistillata*, which also demonstrated that Ca^{2+} incorporation was disproportionately accelerated in high temperature and light levels compared with Sr^{2+} , and as a result, Sr/Ca was inversely related to calcification (Ferrier-Pages et al. 2002).

Cohen and colleagues explored Sr/Ca on a diurnal scale (Cohen et al. 2002; Cohen et al. 2001) and distinguished the Sr/Ca-SST relationship between skeletal material formed during light and dark cycle growth. Sr/Ca values measured in skeletal crystals from *Porites lutea* formed during the day diverged from values in crystals formed during the night at the same temperature with increasing temperature. The daytime values over-predicted the increases in temperature (Cohen et al. 2001). Cohen et al. (2002) studied *Astrangia poculata* which is found in both a hermatypic form (acquiring energy from symbiotic single-celled algae known as zooxanthellae) and an ahermatypic form (having no zooxanthellae). The amplitude of oscillations in the Sr/Ca values was greater in the hermatypic form, and the difference in amplitude between hermatypic and ahermatypic forms was greatest in during the day. The hermatypic Sr/Ca values overreacted to temperature changes, predicting a six degree increase in SST over a three year period, when the SST actually decreased by 0.5 degrees (Cohen et al. 2002). Cohen et al. (2001; 2002) hypothesize that Sr/Ca is affected by calcification rate as a result of kinetic processes which differ diurnally and nocturnally in hermatypic corals (i.e. the activity of algal symbionts).

The kinetic processes are not completely understood, but it is known that both passive and active transport regulate the passage of strontium and calcium ions into the coral skeleton. Active transport of the ions occurs via the Ca^{2+} -ATPase pump. This is a light-activated enzymatic pump which has a higher affinity for Ca^{2+} over Sr^{2+} (Cohen and McConnaughey 2003). Active transport is likely the dominant pathway for transport of these two ions during the day. Nighttime passage is dominated by passive transport, which does not favor one ion over the other, and should thus be driven by ambient

seawater concentrations alone. Therefore, during the day when active transport is dominant, Sr/Ca values should be lower than expected, and Sr/Ca should be lower in more rapidly calcifying corals than in slower calcifiers (Cohen and McConnaughey 2003). Reduced Sr/Ca predicts higher SST in the model equations because of the inverse relationship between Sr/Ca and SST, potentially exaggerating temperature increases. These notions support the results found by Cohen et al. (2001; 2002), Ferrier-Pages et al. (2002), and Reynaud et al. (2004).

The differences in crystals formed during the day versus the nighttime result from differences in coral growth during the diurnal cycle (Cohen et al. 2001; 2002). Extension of the coral's skeleton generally occurs during the night and is the result of granular crystal formation, while daytime growth is mainly thickening of the skeleton and is a result of acicular crystal formation (Cohen and McConnaughey 2003; Cohen et al. 2001). This enables daytime growth to be distinguished from nighttime growth (Cohen et al. 2001). Daytime crystal formation is more rapid than nighttime crystal formation in hermatypic corals due to the energy gained from photosynthesis in the symbiotic relationship with zooxanthellae (Cohen and McConnaughey 2003).

These diurnal patterns in the type and rapidity of growth, combined with daytime photosynthesis by zooxanthellae (Muller-Parker and D'Elia 1997) and the tendency of skeletal accretion to be enhanced by temperature (both day and night), results in density banding on a seasonal scale in many corals (Lough and Barnes 1997). During the winter when the water temperature is lower, corals calcify slower and the skeleton is less dense; during the summer, the water temperature is elevated and solar irradiance is generally elevated, corals calcify quicker, and as a result the skeleton is denser (Lough and Barnes

1990). Growth and density variation could result in seasonal differences in Sr/Ca which do not reflect SST alone. Evidence for this comes from Cohen et al. (2002); daily variation in Sr/Ca between the hermatypic and ahermatypic corals was greater in the summer than in the winter.

Bell et al. (2011a) found preliminary evidence of seasonal variation in the Sr/Ca-SST relationship in Guam corals. (Guam's seasons are better defined as wet season and dry season, rather than summer and winter.) The correlation coefficient between SST and Sr/Ca in the wet season (June-September) was nearly half that of the dry season (December-March) in a single core collected from a *Porites lobata* colony. During the wet season SST is generally higher, on average 29.3 degrees Celsius, compared to 27.7 degrees Celsius during the dry season. It is therefore expected that coral growth and calcification are more rapid during the wet season than the dry season. This is likely complicated, however, by the seasonal heavy rains resulting in turbid plumes of terrestrial sediment and reduced light which could affect the activity of zooxanthellae. An additional complication may be bleaching events (Rosenfeld et al. 2006), which increase in frequency with increasing SST, leading to more stress for corals and as a result slower growth.

The main objective of the present study is to further explore the Sr/Ca-SST relationship in the corals of Guam and determine how growth parameters may explain some of the variation which is not consistent with SST. Briefly, this will be accomplished by exploring multiple cores of a single species from three sites, measuring Sr/Ca as well as growth parameters, and aligning the data sets with instrumental SST records.

There are multiple growth parameters which are important in determining the effect of growth on the Sr/Ca-SST proxy. First, linear extension rate, measured as growth along the vertical plane, has been found to correlate linearly with SST and inversely with Sr/Ca (Lough and Barnes 2000). Second, skeletal density, a measure of the thickness of a given part of the skeleton, varies seasonally and is generally positively related to SST and linear extension rate (Lough and Barnes 1990). The product of linear extension rate and density gives a value of calcification. Calcification is generally positively correlated with SST (Lough and Barnes 2000) and inversely related to Sr/Ca (Reynaud et al. 2004; Ferrier-pages et al. 2002). Another parameter which can be measured is tissue thickness which can have an effect on sub-annual banding (Barnes and Lough 1993). This is calculated by measuring the distance between dissepiments (structures that form a floor for the living tissue of the polyp) in the skeleton. Here, the focus is on the first three parameters, which are easily calculated from x-ray (Lough and Barnes 2000; Barnes and Lough 1993) or CT scan images and their relation to SST and Sr/Ca.

The present study evaluates the relationships outlined in Fig. 1.1, by meeting the following objectives: 1.) determine how coral growth has varied over the last 30 years by analyzing density banding in multiple coral cores; 2.) determine the relationship between sea surface temperature (SST) and Sr/Ca measured in the cores and SST and coral growth; 3.) determine whether including coral growth parameters can improve the accuracy of the Sr/Ca-SST model; and 4.) discuss potential environmental factors which may influence the accuracy of the Sr/Ca-SST proxy. As a result of uncovering some unexpected Sr/Ca-SST relationships, the potential for other metal/Ca-SST proxies is also briefly explored.

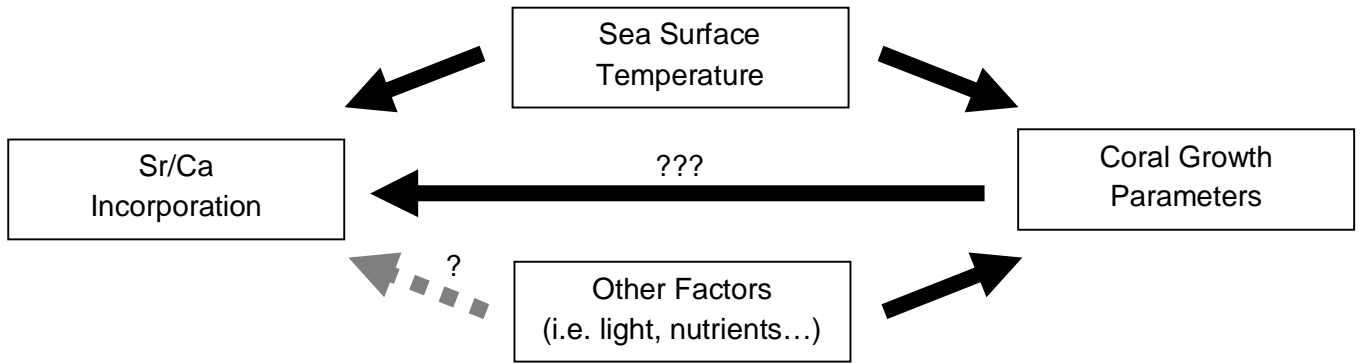


Figure 1.1 Relationship model between SST, Sr/Ca, and coral growth. Arrows indicate dependencies between factors (solid = direct effect, dashed = indirect effect). Question marks indicate potential relationships which will be assessed in the proposed study.

Chapter 2: Methods

Coral Sampling

Cylindrical cores were extracted from six corals, two at each of three sites (Asan, Agat, and Apra Harbor; Fig 2.1) between April 26 and April 28, 2012. These locations were selected due to their proximity to War in the Pacific National Historical Park which was the target area of the grant funding the project. Each specific coral that was selected is among the tallest living massive *Porites* colonies available in each area in order to provide the longest climate record possible. Metadata for each colony can be found in Appendix A. Photographs of the overall morphology of the coral (Appendix A) and a skeleton chip at least three centimeters in diameter were collected for species identification. Professor Richard Randall confirmed the identification of all six corals as *Porites lutea*.

One core, eight centimeters in diameter, was extracted from each coral using a pneumatic drill. The specifications of the drill can be found in Bell et al. (2011b). Cores were extracted from the center of the highest part of the coral colony through the vertical plane. The length of the cores ranged from about 50 cm to 136 cm.

After the cores were collected, each core was rinsed in freshwater to remove debris from the drilling. The cores were then measured and photographed. Each core was dried overnight, packed in bubble wrap, and transported to the USGS headquarters in Santa Cruz, CA by Dr. Nancy Prouty. From Santa Cruz, the cores were shipped and transported for density and metal analyses as discussed below.

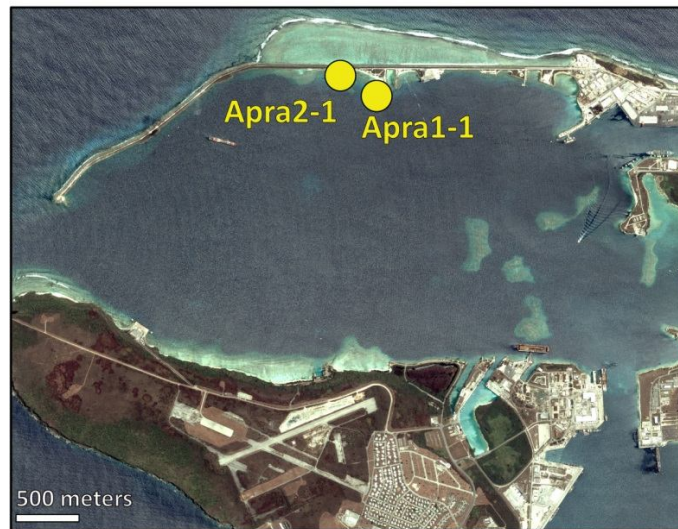


Figure 2.1 Maps of coring sites (awaiting access to ArcGIS for map of Guam with sites)

CT Scan and Coral Growth Parameters

All cores were shipped intact to Woods Hole Oceanographic Institution (WHOI) in Woods Hole, Massachusetts to the laboratory of Dr. Anne Cohen for determination of the skeletal density, annual linear extension rate and annual calcification rate. Cores were imaged using a Siemens Volume Zoom Helical Computerized Tomography (CT) Scanner set at 350mAs and 120kV as described in Cantin *et al.* (2010) and Saenger et al (2009). Cores were reconstructed using an ultra-high bone algorithm and virtual image manipulation to produce complete 3-D images (Cantin *et al.* 2010).

Skeletal density and annual linear extension rate were calculated for each core from 3.03-mm thick virtual slices from the mean projection of the reconstructed 3-D images, using ImageJ® software (available at <http://rsbweb.nih.gov/ij/download.html>). Greyscale values were collected at an interval of approximately 0.33 mm along two 3-mm wide transects in each virtual slice. Coral standards of known density were scanned along with the cores and analyzed in ImageJ to establish a linear relationship between density and the greyscale values. Greyscale values from the cores were converted to skeletal density values using this relationship. Annual linear extension rate was calculated as the distance between lowest density values in successive high-low density band pairs.

The average of all density values within each band pair was considered the average annual density. Average annual calcification was calculated by multiplying the average annual density by the annual extension rate for each band pair. Values from the two transects from each core were averaged to obtain a single value for annual density, linear extension rate, and calcification for each year analyzed for a core. Additional transects were run on short sections of each core to assess within core variability. Bands

pairs were assigned to years by assuming that the first complete band pair from the top of each core was 2011 and naming each successive band pair the preceding year.

Linear extension rates for the analyzable extent of each core, along with raw high-resolution density data, annual density data, and annual calcification rates for the past 26 to 31 years were received via email directly from Dr. Anne Cohen of WHOI. Datasets varied in length due to the number of bands that fit into each image (high-resolution density measurements were only made for only the first few images of each core) and the number of analyzable band in each core.

Metal/Ca Ratio Measurements

The coral cores were taken to Australia National University where a suite of metal/Ca ratios were measured along each core by Dr. Nancy Prouty of USGS using laser ablation inductively coupled mass spectrometry (LA-ICP-MS). Briefly, LA-ICP-MS is an automated technique where a laser is moved along a programmed path, removing samples at a prescribed interval to be introduced to the ICP-MS analysis. This technique is considered one of the most efficient ways to measure Sr/Ca (Fallon *et al.* 2001).

Prior to the LA-ICP-MS procedure, the slabs were cut into sub-sections of approximate 95 by 25 mm using a diamond blade saw. Each sub-section was placed individually in the sealed chamber of the machine under helium atmosphere. In order to ensure that no debris from the cutting process polluted the sample, the top 5-10 μm of each slab to be measured was ablated using a 3 cm by 1cm masking laser beam (40 x 500 μm rectangular aperture) at a pulse rate of 10Hz. This process is described in Wyndham *et al.* (2004).

The molar concentration of ^{11}B , ^{25}Mg , ^{84}Sr , ^{137}Ba , ^{138}Ba , ^{238}U , and ^{43}Ca were measured at intervals of 0.22 mm along the major growth axes determined in the CT analysis for each coral. Sample ablation was achieved using a 40 by 400 μm laser at a pulse rate of 40 $\mu\text{m s}^{-1}$ at 5 Hz. The data were standardized using the glass standard National Institute of Standards and Technology (NIST) 614 and a pressed-powder coral disk for which metal/Ca ratios were determined by isotope dilution ICP-MS (Fallon *et al.* 2001). Molar concentration of each metal was translated into a metal/Ca mole to mole ratio. Replicate and occasionally triplicate transects were measured to determine within core variability. Data were background and drift corrected, smoothed using a 10-point running median to reduce volume, and filtered to remove spikes resulting from accumulation of ablated material.

Sea Surface Temperature and other Environmental Time Series

Monthly SST data from the Hadley dataset, available at one degree resolution, was downloaded from the National Oceanic and Atmospheric Administration (NOAA) Division of Environmental Research (<http://coastwatch.pfeg.noaa.gov/erddap/griddap/erdHadISST.html>) for the area between 13 to 14°N and 144 to 145°E. Bell *et al.* (2011a) found that, of the publically accessible SST datasets, Hadley best matched actual temperatures measured on Guam's reefs. Despite the conclusions of that study, spatial variation in SST was further considered by comparing the Hadley data to the SST data from the Scripps Coastal Data Information Program (<http://cdip.ucsd.edu/>) wave buoy off the coast of Ipan, Guam and HOBO temperature loggers placed on the Asan and Agat reef flats for several months as part of another project. Hadley was found to be consistent with the wave buoy data, verifying its

validity for this reconstruction project. However, both datasets underestimate the total temperature range experienced on the reef flats by almost 3°C (Appendix B).

Additional environmental datasets were located and obtained from various sources in order to determine other drivers for variability in the coral data. Total monthly rainfall data measured at the National Weather Service station in Tiyan, Guam were downloaded from the Western Regional Climate Center (<http://www.wrcc.dri.edu/summary/climsmhi.html>) for 1982 to 2012. Mean sea level measurements from Apra Harbor, Guam were downloaded from NOAA (<http://www.tidesandcurrents.noaa.gov>) for 1996 to 2012. Monthly averages for wave height, average period, and peak period were downloaded from the Scripps CDIP wave buoy in Ipan, Guam (<http://cdip.ucsd.edu/>) for 2003 to 2012. Monthly data from the Multivariate El Niño/Southern Oscillation Index (MEI) were downloaded from NOAA's Earth System Research Laboratory (<http://www.esrl.noaa.gov/psd/enso/mei/>) for 1950 to 2012.

Determination of Chronology

To explore relationships between environmental data and parameters measured in the coral core, it was necessary to assign specific dates to each individual measurement. Raw density data were assigned dates based on the density band assignment determined in the CT analysis (Crook et al 2013). The first density value in each annual band pair (the lowest density measurement in the low density band) was assigned to the lowest SST month in the corresponding year. This assignment was made for the two transects for each core separately. Each year, therefore, had one tie point with which to align the chronology for the remaining density values. These chronologies were applied using the

Ager program of ARAND (a free software package developed for paleontological time series, available at <http://www.ncdc.noaa.gov/paleo/softlib/arand/arand.html>).

The density-derived chronologies were revised for use with the LA-ICP-MS data when metal/Ca revealed clear annual structure. Although the position of the LA-ICP-MS transects were based on the CT data, the internal topography of each core was complex. As a result, the exact position of density bands crossed by the LA-ICP-MS transects are expected to be slightly different than in the transects analyzed for the density measurements. Therefore, where Sr/Ca values showed visible annual structure, as in the Asan1-1 and Asan2-1 samples, chronologies were refined based on Sr/Ca values. The highest Sr/Ca value for the year was assigned to the lowest SST month (most commonly February) and the lowest Sr/Ca value was assigned to the highest SST month for the year (most commonly August). These two tie points were used to assign the remaining values to a date in the Ager program. Sr/Ca data for Agat1-1 and Apra2-1 lacked apparent annual structure, so the density-derived chronology was applied without revision using Ager.

All density and LA-ICP-MS data were smoothed to evenly-spaced monthly values using the Timer software of ARAND. Through this function, each data point is interpolated linearly from the nearest values using a specified time-step, in this case 0.8333 (1/12) years. Annual datasets were obtained for LA-ICP-MS data by averaging all monthly data points for a given metal/Ca ratio within one calendar year. Annual linear extension rates, density values and calcification rates were used directly from the dataset received from WHOI.

Sr/Ca-SST Model Determination and Analysis

The monthly Sr/Ca datasets for each core were regressed with the Hadley SST data to create a unique linear model equation for each core. That linear equation served as a Sr/Ca-SST calibration equation. The slope and intercept of all significant Sr/Ca-SST regression equations were compared between sites and with published Sr/Ca-SST calibration equations. The relationship between skeletal density and SST were also assessed using a simple regression test between monthly skeletal density values and sea surface temperature. Monthly Sr/Ca was then regressed against monthly skeletal density to determine possible dependency. All regression analyses were performed in Statview.

In order to determine whether adding skeletal density to the Sr/Ca-SST regression model could improve its accuracy, monthly Sr/Ca for each core was regressed against both SST and skeletal density in a multiple regression test. Regression coefficients and p-values were compared between the various model equations for each core and between cores. These regression analyses were repeated with annual Sr/Ca values, average annual density values, annual linear extension rates, and annual calcification rates.

Analysis of other metals and environmental factors

In response to finding weak seasonal signals in the Sr/Ca data and weak relationships between Sr/Ca, SST, and growth parameters in some of the cores, numerous other datasets were analyzed in order to reveal factors confounding the Sr/Ca-SST relationship. The additional monthly metal/Ca ratio time series obtained from the LA-ICP-MS analysis (Ba/Ca, Mg/Ca, B/Ca and U/Ca) were explored visually and through correlation z-tests for similarities with the Sr/Ca datasets and each other metal/Ca dataset. Furthermore, Empirical Orthogonal Function (EOF) analysis was performed in

MATLAB (by Dr. Nancy Prouty) to extract underlying structure in the five metal/Ca ratio monthly time series for each core. Individual metal/Ca datasets and the first EOF for each core were regressed against SST to determine whether SST is a major driver in the incorporation of any of these metals. Metal/Ca ratios were also regressed against the growth parameters. Any metal/Ca ratio which was well-correlated with SST was regressed with SST and the growth parameters in multiple regression tests, to determine whether that metal/Ca ratio may be a more appropriate proxy than Sr/Ca.

All available environmental datasets were also compared to each Sr/Ca dataset using simple and stepwise regression analyses for monthly and annual time series. These were used to determine whether any of the other environmental parameters might be influencing and perhaps trumping the influence of SST and the coral growth factors in the incorporation of strontium.

Chapter 3: Results

Coral Growth and Calcification

Of the six coral cores collected, four showed annual density bands which were distinguishable in the CT scan data. The other two cores (Agat2-1 and Apra1-1) were excluded from the analysis because the density banding was too complicated to assign a chronology (determined by Dr. Anne Cohen at WHOI).

Density band pairs were numbered and dated as described in Chapter 2. The longest record recovered from the cores was Asan1-1, from which 111 annual density bands were analyzed. One hundred and one bands were analyzed from Agat1-1, 33 from Apra2-1 and 33 from Asan2-1. The number of bands is equivalent to the approximate age of the bottom of each core, though in most cases, this is not equivalent to the age of the coral from which it was collected as we were unable to obtain a core from the full height of the coral due to technical or time restrictions of the drilling operation.

Overall, the range of skeletal density was similar in all four cores (Table 3.1); however, differences at a given point in time, even on the annual scale, were great between cores (Fig 3.1).

Table 3.1. Descriptive statistics for monthly skeletal density values 1985-2010. All values are in grams per cubic centimeter.

Site	Mean	Min	Max	SD
Agat1-1	1.106	0.857	1.373	0.099
Apra2-1	1.136	0.971	1.345	0.071
Asan1-1	1.184	0.839	1.475	0.129
Asan2-1	1.275	0.890	1.532	0.102

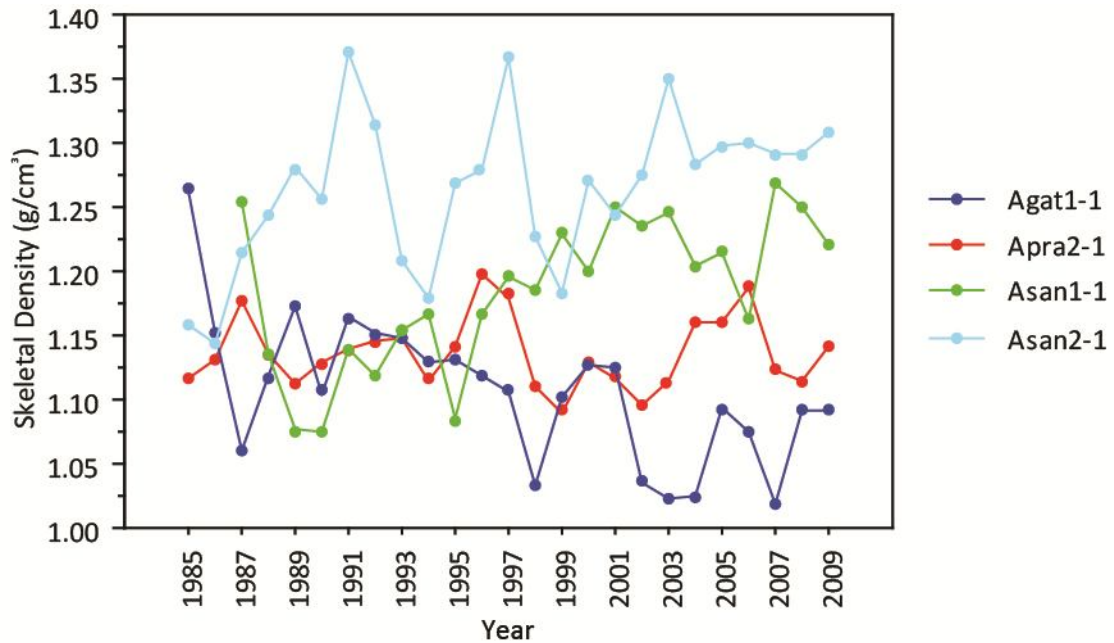


Figure 3.1 Annual skeletal density measurements 1985-2010

The average linear extension rate for the cores was 1.01 ± 0.20 cm/yr which is comparable to massive *Porites* records from Guam and the western Pacific region (Asami *et al.* 2005, Bell *et al.* 2011a). Asan1-1 grew slowest (0.92 ± 0.13 cm/yr), followed by Apra2-1 (1.18 ± 0.12 cm/yr), Asan2-1 (1.27 ± 0.12 cm/yr) and Agat1-1 (1.28 ± 0.14 cm/yr). Each annual linear extension rate record was distinct, showing little congruency between corals (Fig 3.2). Calcification rate varied between sites similarly to linear extension rate (Fig 3.3). Average calcification rate for Asan1-1 was significantly lower (t-tests $p < 0.0001$) than for the other three corals which did not differ significantly from one another.

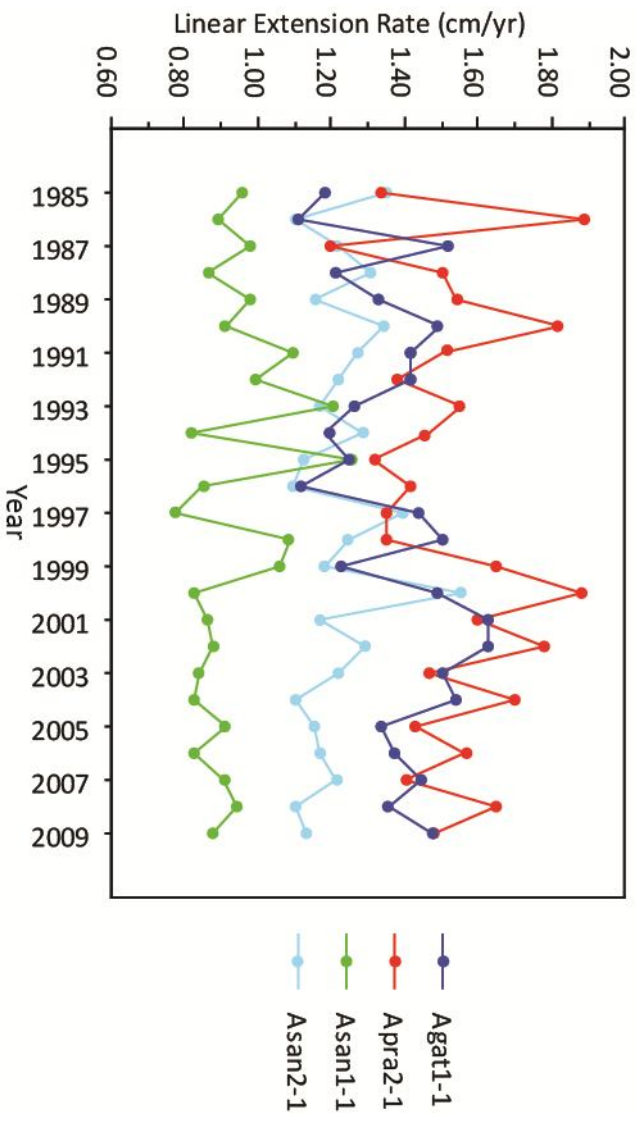


Figure 3.2 Annual linear extension rates 1985-2010

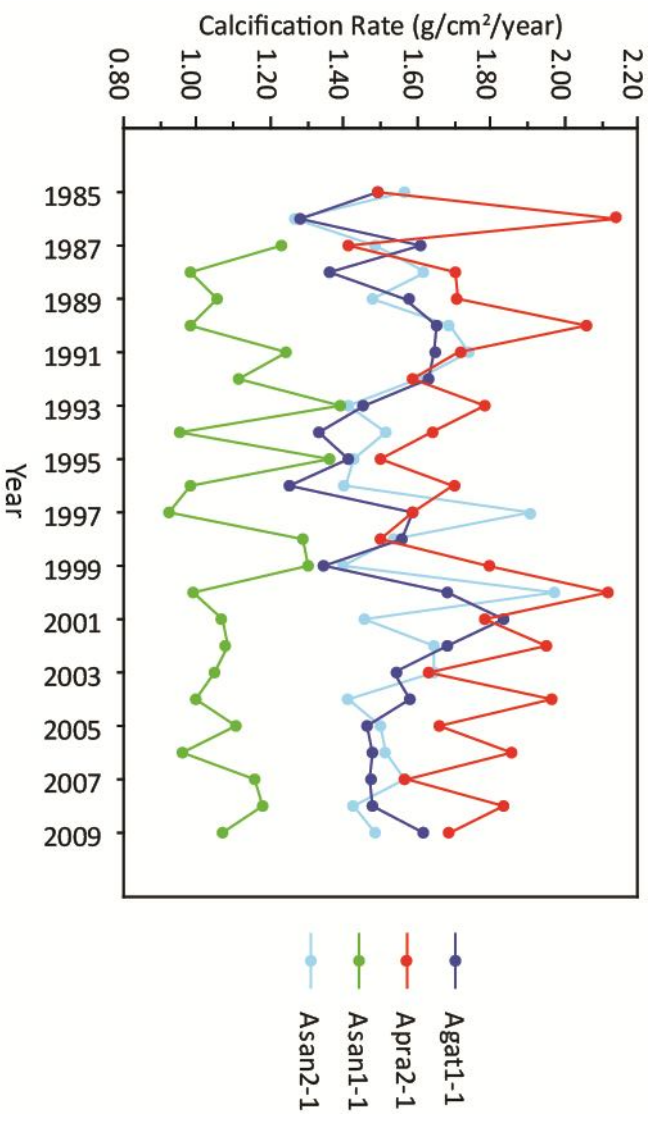


Figure 3.3 Annual calcification rates 1985-2010

Sr/Ca

The raw high-resolution LA-ICP-MS Sr/Ca measurements showed great variability within and between replicate tracks (Appendix C). This type of variation is expected with high-resolution data like that from LA-ICP-MS because of microscopic skeletal structure variations that are typically undetected by lower resolution sampling methods (Cohen and McConnaughey 2003). After applying an eleven-point moving average to the raw data, a more defined structure was revealed in all cores. In Asan1-1 and Asan2-1, the annual nature of that structure was apparent, whereas in Agat1-1 and Apra2-1, the structure did not vary consistently in an annual cycle.

The data were matched to chronologies and resampled at a monthly interval as discussed in Chapter 2. Analyses were limited to the timeframe 1985-2010 because Sr/Ca for this time period was sampled and replicated in each core. 2010-2011 data were also available for all cores, but was excluded due to apparent spikes in the Sr/Ca data resulting from sampling the tissue layer.

Mean Sr/Ca values were similar between the full raw datasets and the smoothed, resampled data except for a notable increase in Sr/Ca for Asan1-1 which resulted from excluding a concentrated section of low Sr/Ca values which occurred in the portion of the core corresponding to the 1950s (Table 3.2). Mean Sr/Ca values were similar in Apra2-1 to the Apra Harbor core in Bell *et al.* 2011a, although the range of values and standard deviation were notably greater in Apra 2-1, likely due to the differing Sr/Ca sampling methods.

Table 3.2 Descriptive statistics for raw Sr/Ca measurements, Sr/Ca values after processing, and Sr/Ca values from Bell *et al.* 2011a. All values are in moles (Sr mol/Ca mol).

Core	Raw				Processed			
	Mean	SD	Max	Min	Mean	SD	Max	Min
Agat1-1	0.0091	0.0002	0.0101	0.0078	0.0091	0.0001	0.0095	0.0087
Apra2-1	0.0089	0.0002	0.0096	0.0082	0.0089	0.0001	0.0092	0.0086
Asan1-1	0.0089	0.0003	0.0102	0.0061	0.0091	0.0002	0.0095	0.0088
Asan2-1	0.0089	0.0003	0.0107	0.0065	0.0089	0.0001	0.0092	0.0085
Bell <i>et al.</i> 2011	0.0089	0.0001	0.0092	0.0087	-	-	-	-

The structure of the annual Sr/Ca time series are surprisingly different between the cores (Fig 3.4). Notable differences include a spike in Sr/Ca in Agat1-1 around 2002 and an increasing trend between 1989 and 1994 in Asan1-1 which are absent from the other time series. Annual average Sr/Ca values are consistently lower in Apra2-1 and Asan2-1 compared to the other two corals.

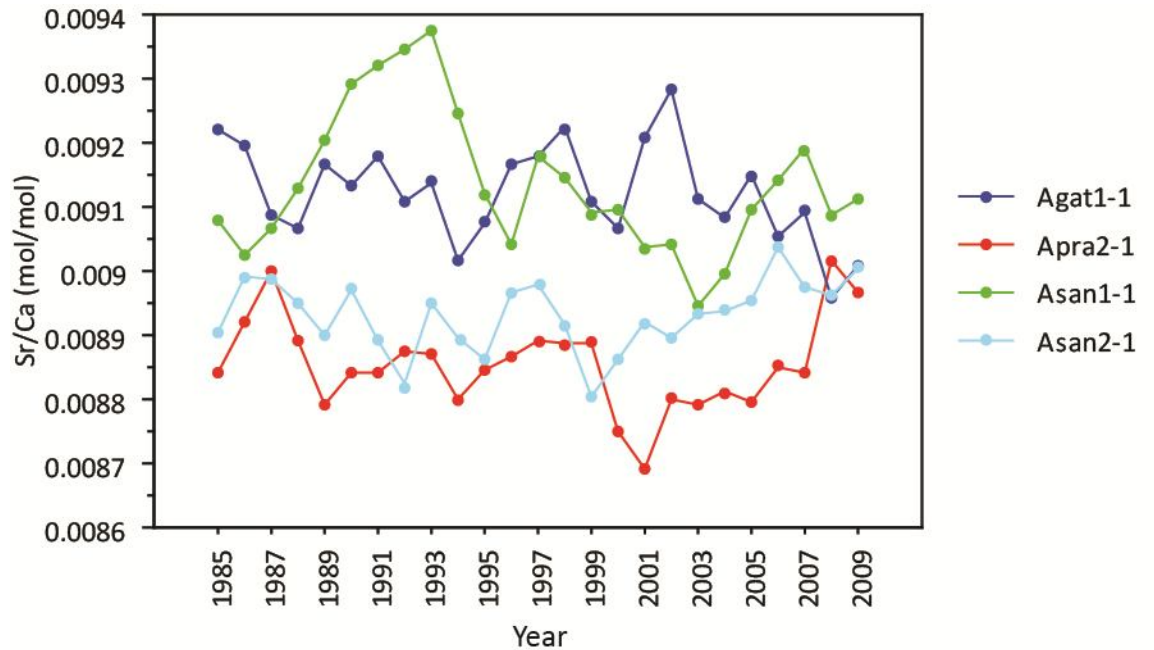


Figure 3.4 Annual Sr/Ca measurements 1985-2010

Sea Surface Temperature Model

The relationship between monthly Sr/Ca and SST is surprisingly weak or absent in the four cores analyzed here (Fig 3.5-8). Asan1-1 displays the strongest relationship (Fig 3.7) with an R^2 of 0.404 ($p < 0.0001$) for the monthly time series and 0.489 ($p < 0.0001$) for the annual time series. This is lower than the 2011 analysis of a core from Apra Harbor, Guam which had an R^2 of 0.549 for a monthly times series (Bell *et al.* 2011a) and remarkably lower than others reported in literature, with R^2 values as high as 0.96 (Correge 2006). The relationship for the Asan2-1 core is weaker (Fig 3.8), but still significant ($R^2=0.251$, $p < 0.0001$) for the monthly time series. However, the annual trend in Sr/Ca and SST, was not significantly related for Asan2-1. Agat1-1 and Apra2-1 monthly and annual Sr/Ca values showed no significant relationship to the SST time series (Fig 3.5 and Fig 3.6).

The range in annual average SST was $<1^\circ\text{C}$, 28.06°C to 29.05°C , with a mean of $28.74^\circ\text{C} \pm 0.236^\circ\text{C}$, and a majority of the years fell in the upper half of the temperature range. Notably, between 1989 and 1994 mean temperatures were colder and on a decreasing trend. The Sr/Ca-SST relationship in the annual time series for Asan1-1 (Fig 3.7 D) was visibly driven by these lower temperature years, which also exhibited increasing annual Sr/Ca values. When these years are examined separately (Fig 3.9), the resulting regression analysis reveals a very strong Sr/Ca-SST relationship with an R^2 of 0.948 ($p < 0.0001$). Apra2-1 also shows a significant relationship between Sr/Ca and SST for those years ($R^2 = 0.897$, $p = 0.0042$).

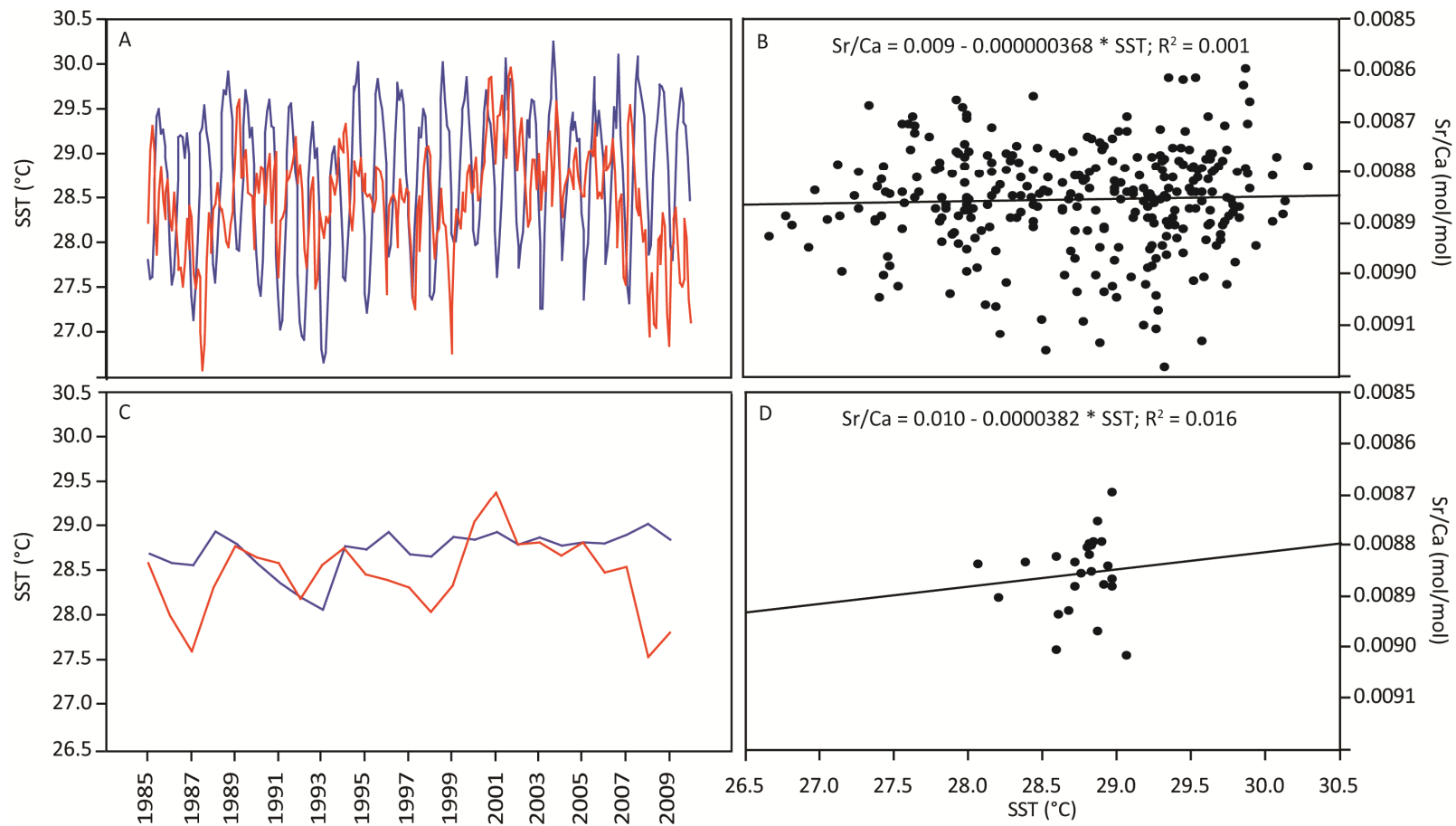


Figure 3.5 Apra2-1 Sr/Ca-SST analysis. A.) 1985-2010 monthly time series for SST (blue line) and Sr/Ca (red line) and B.) a regression plot of the same time series. C.) 1985-2010 annual time series for SST (blue line) and Sr/Ca (red line) and D.) a regression plot of the same time series.

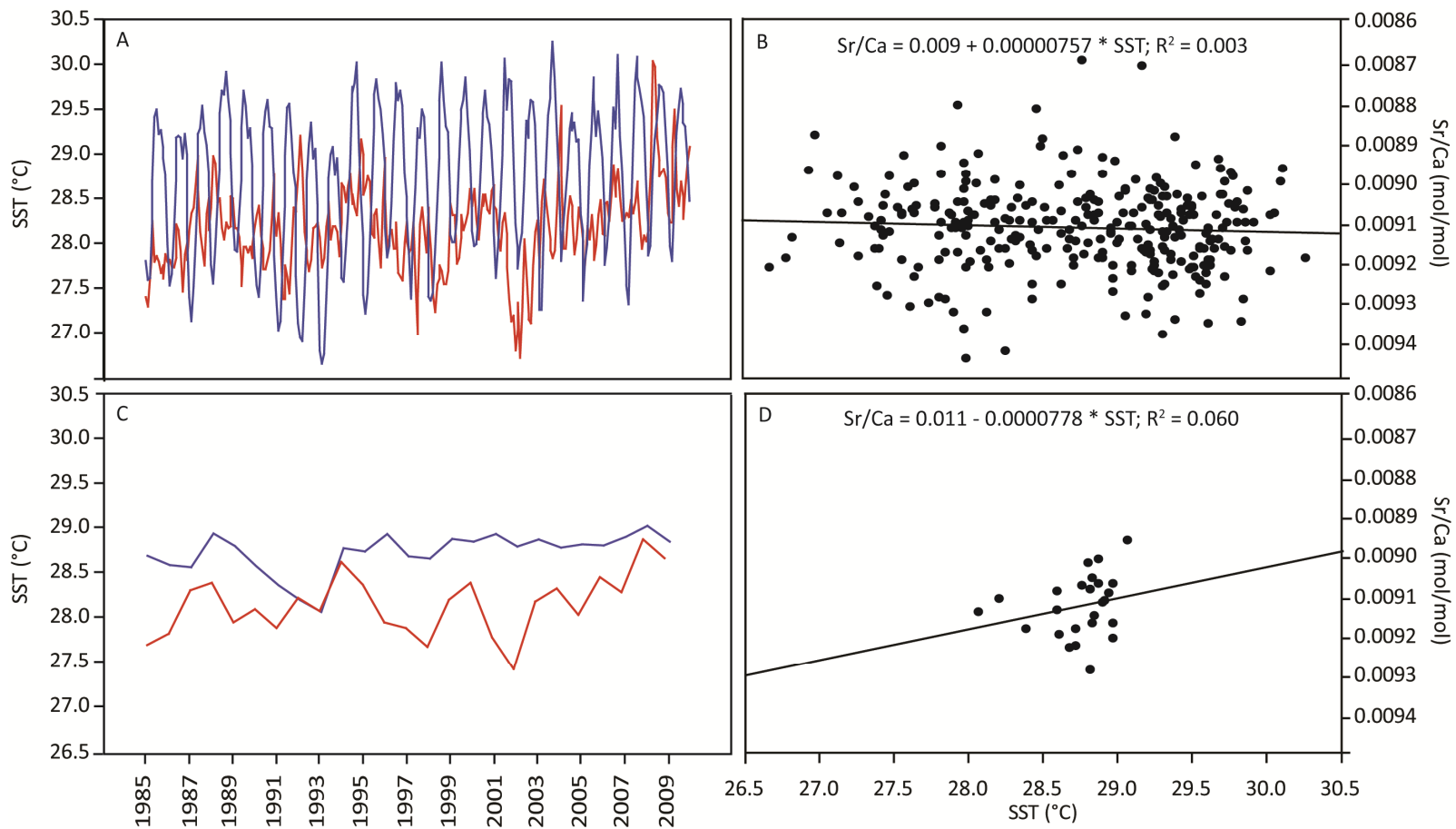


Figure 3.6 Agat1-1 Sr/Ca-SST analysis. A.) 1985-2010 monthly time series for SST (blue line) and Sr/Ca (red line) and B.) a regression plot of the same time series. C.) 1985-2010 annual time series for SST (blue line) and Sr/Ca (red line) and D.) a regression plot of the same time series.

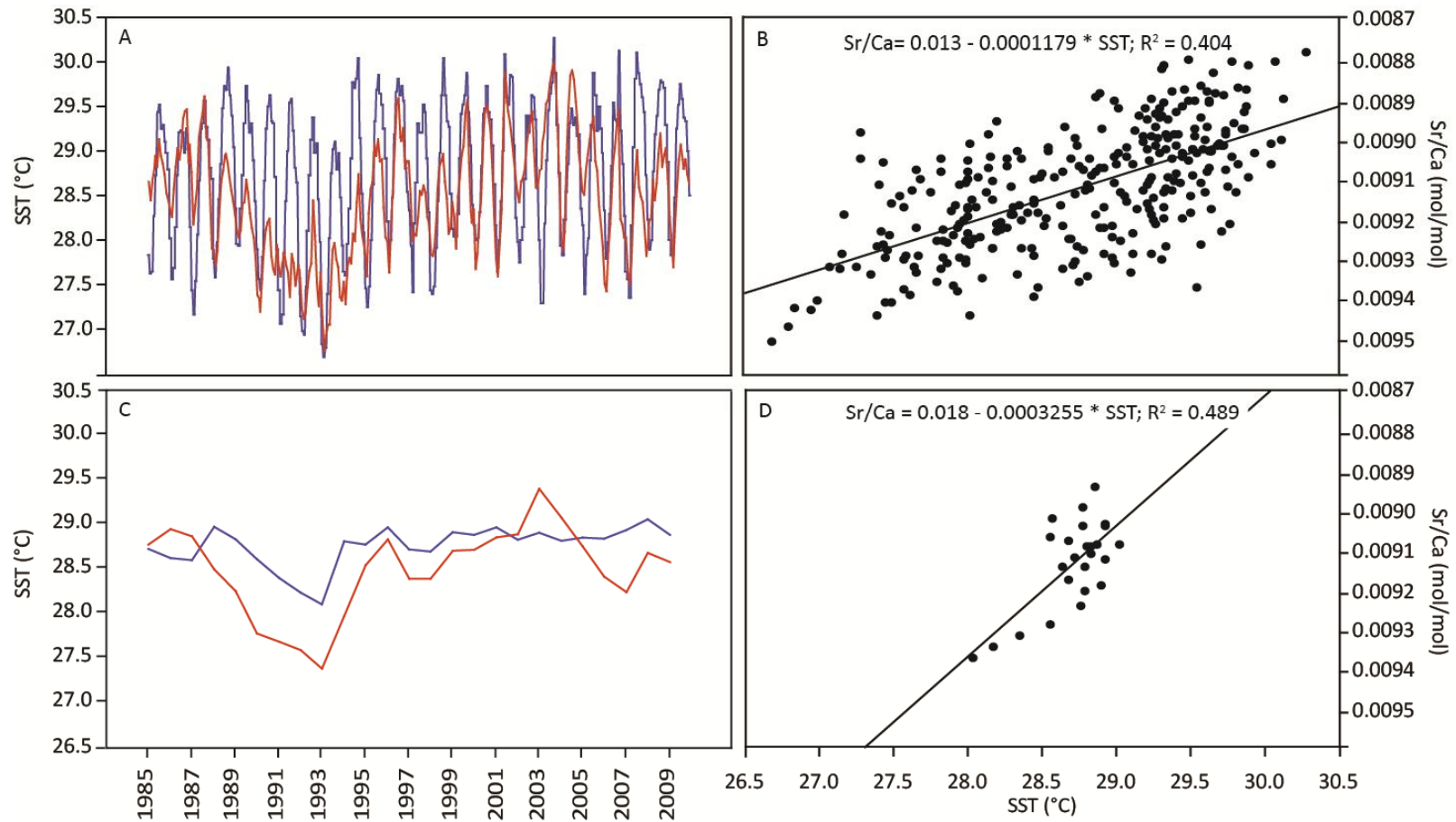


Figure 3.7 Asan1-1 Sr/Ca-SST analysis. A.) 1985-2010 monthly time series for SST (blue line) and Sr/Ca (red line) and B.) a regression plot of the same time series. C.) 1985-2010 annual time series for SST (blue line) and Sr/Ca (red line) and D.) a regression plot of the same time series.

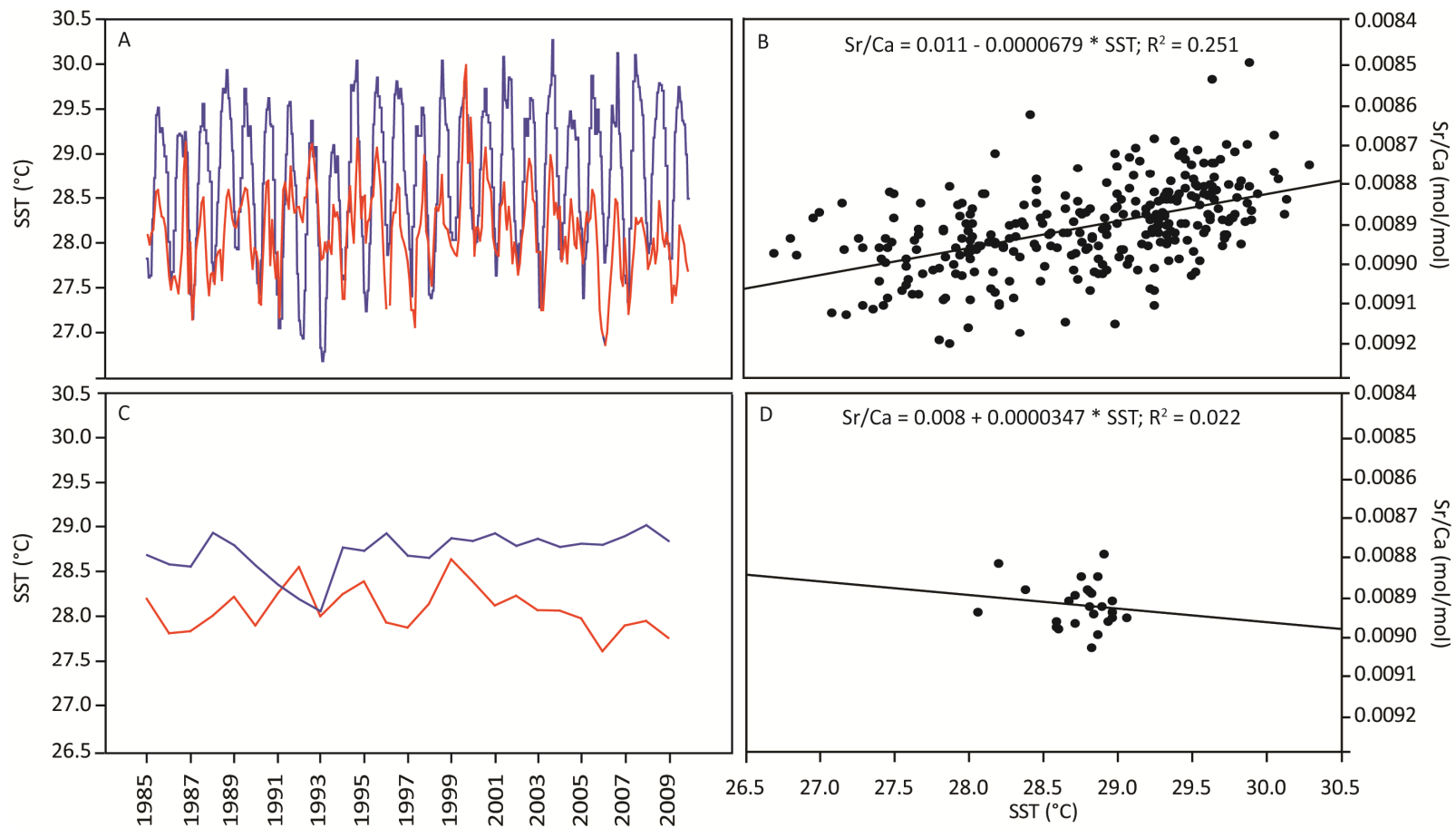


Figure 3.8 Asan2-1 Sr/Ca-SST analysis. A.) 1985-2010 monthly time series for SST (blue line) and Sr/Ca (red line) and B.) a regression plot of the same time series. C.) 1985-2010 annual time series for SST (blue line) and Sr/Ca (red line) and D.) a regression plot of the same time series..

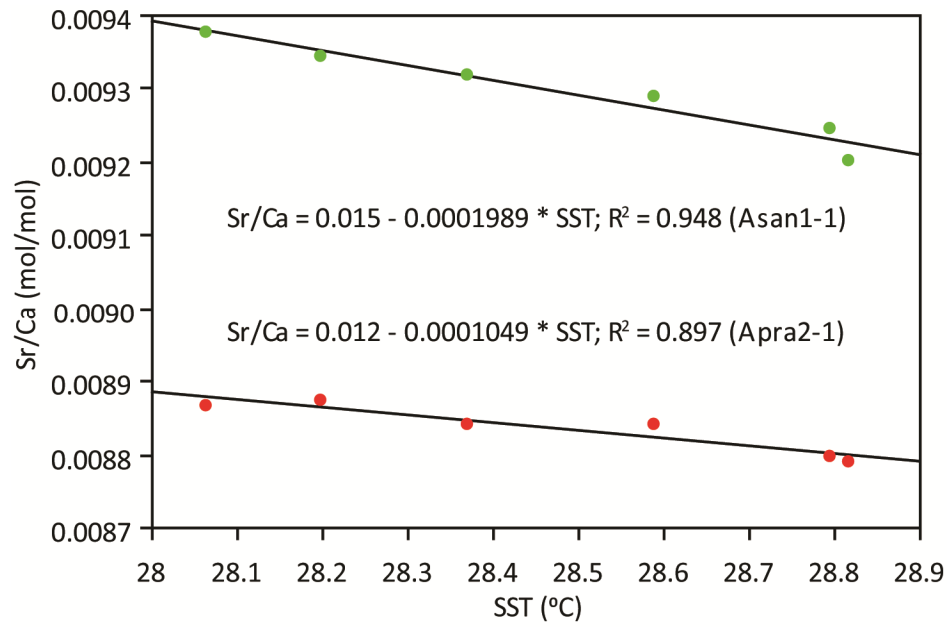


Figure 3.9 Regression plots for annual Sr/Ca and SST 1989-1994 for Apra2-1 and Asan1-1.

Regression analyses for seasonal data do not reveal the predicted relationships (Table 3.3). The relationship between Sr/Ca and SST for all dry months (December-March 1985-2010) and all wet months (June-September 1985-2010) is insignificant for each of the four cores. Wet season temperature averages and dry season temperature averages are each significantly related for Asan1-1. However, the relationships are weaker than for the annual averages, and the wet season relationship is stronger than that of the dry season, which is contradictory to the proposed hypotheses.

Table 3.3 Regression coefficients (R^2) for Sr/Ca and SST for all months, dry months (Dec-Mar), wet months (Jun-Sep), annual averages and wet and dry season averages. * Indicates p-value <0.05 * Indicates p-value <0.0001.**

Site	All Months	Dry Months	Wet Months	Annual Avg	Wet Avg	Dry Avg
Asan1-1	0.404***	0.200	0.180	0.489***	0.053	0.035
Asan2-1	0.251***	0.015	0.051	0.022	0.015	0.016
Apra2-1	0.002	0.011	0.031	0.016	0.464***	0.315*
Aga1-1	0.003	0.004	0.055	0.062	0.006	0.009

The regression equation relating monthly Sr/Ca to SST is $Sr/Ca * 1000 = 12.523 - 0.118 * SST$ for Asan1-1 and $Sr/Ca * 1000 = 10.883 - 0.068 * SST$ for Asan2-1. The Asan2-1 equation is similar to the mean equation in Correge's review of published Sr/Ca-SST equations from massive *Porites* around the world ($Sr/Ca * 1000 = 10.553 - 0.0607 * SST$). The equation for Asan1-1 has a steeper slope and greater intercept than all equations published in the review. The slope is even steeper for the annual Asan1-1 data ($Sr/Ca * 1000 = 18.49 - 0.325 * SST$). All three regression equations from the new Guam sites had steeper slopes and greater intercepts than the equation from 2011 study in Apra Harbor (Bell *et al.* 2011, $Sr/Ca * 1000 = 9.92 - 0.037 * SST$) (Fig 3.10).

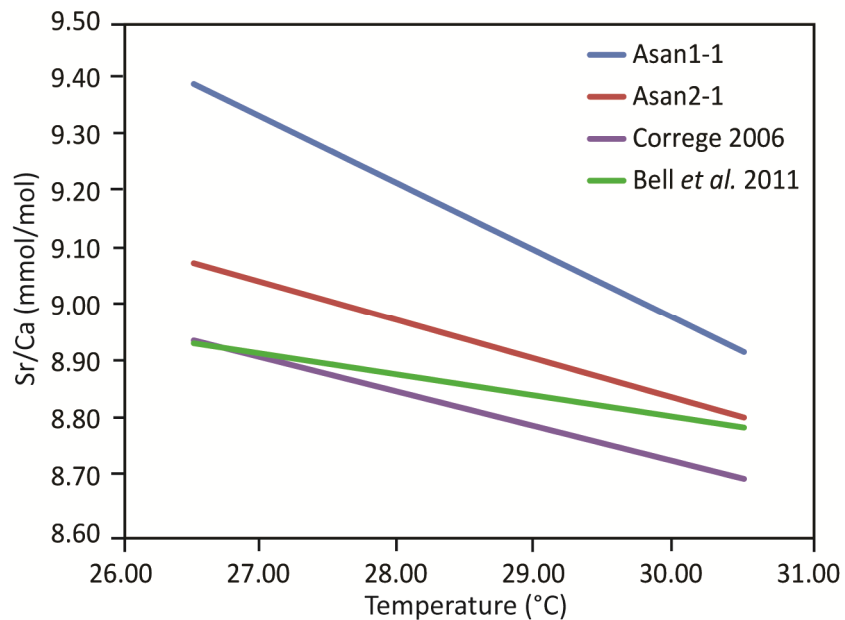


Figure 3.10 Sr/Ca-SST calibration equations for Asan1-1 and Asan2-1 monthly datasets compared with the average *Porites* equation presented by Correge (2006) and that from Bell *et al.* (2011a).

Growth-Dependent Sea Surface Temperature Model

Monthly Sr/Ca was weakly, but significantly, correlated with skeletal density in Agat1-1 and Asan2-1. A slightly stronger relationship was present in Asan1-1, and no significant relationship was found in Apra2-1 (Table 3.4).

Table 3.4 Simple regression results for monthly Sr/Ca and skeletal density 1985-2010

Sr/Ca vs. Density (Monthly)				
Site	R ²	P-value	Slope	Intercept
Agat1-1	0.026	0.0050	0.0002	0.009
Apra2-1	0.002	0.4422	0.0001	0.009
Asan1-1	0.223	<0.0001	-0.0010	0.010
Asan2-1	0.039	0.0006	-0.0002	0.009

Skeletal density was significantly correlated with SST in all cores; however, the variation in density explained by SST was under 10% in Agat1-1 and Apra2-1 and under 30% in the other two cores (Table 3.5).

Table 3.5 Simple regression results for monthly skeletal density and SST 1985-2010

Density vs. SST (Monthly)				
Site	R ²	P-value	Slope	Intercept
Agat1-1	0.083	<0.0001	0.0360	0.080
Apra2-1	0.086	<0.0001	0.0260	0.394
Asan1-1	0.297	<0.0001	0.0870	-1.304
Asan2-1	0.223	<0.0001	0.0600	-0.452

When considered as a factor in the Sr/Ca-SST regression model using a multiple regression test, monthly skeletal density improves the ability of the model to predict SST very slightly for all of the cores (Table 3.6). However, the associated t-tests show that

only the improvements to the Asan1-1 equation are significant. When Sr/Ca is regressed against the same two independents using a stepwise regression test, density only remains a significant contributor to the Asan1-1 calibration equation, reinforcing the multiple regression results.

Table 3.6 Multiple regression results for monthly Sr/Ca, SST and skeletal density 1985-2010

Sr/Ca vs. SST and Density (Monthly)						
Site	Original R ²	R ²	P-value	Partial Slope SST	Partial Slope Density	Intercept
Agat1-1	0.003	0.026	0.0192	0.000001	0.00017	0.009
Apra2-1	0.002	0.004	0.5610	-0.000006	0.00008	0.009
Asan1-1	0.404	0.454*	<0.0001	-0.000107	-0.00019	0.012
Asan2-1	0.251	0.253	<0.0001	-0.000071	0.00005	0.011

Annual Sr/Ca was not significantly related to linear extension rate, skeletal density, or calcification rate in any core except Asan1-1, which showed a small positive relationship between Sr/Ca and skeletal density and between Sr/Ca and linear extension rate (Table 3.7-9). The three growth parameters were similarly related with SST. No significant correlations between annual growth parameters and SST are found for Agat1-1, Apra2-1 and Asan2-1. All three parameters were significantly correlated with SST for Asan1-1, although again the variability explained is under 30% (Table 3.9-11).

Table 3.7 Simple regression results for annual skeletal density, Sr/Ca and SST 1985-2010

Site	Sr/Ca vs. Density (Annual)				Density vs. SST (Annual)			
	R ²	P-value	Slope	Intercept	R ²	P-value	Slope	Intercept
Agat1-1	0.026	0.4370	0.002197	0.009	0.106	0.1127	-0.077	3.311
Apra2-1	0.049	0.2898	0.001000	0.008	0.027	0.4349	-0.019	1.694
Asan1-1	0.343	0.0033	-0.001000	0.010	0.171	0.0496	0.098	-1.643
Asan2-1	0.012	0.6044	0.000103	0.009	0.003	0.7906	0.014	0.861

Table 3.8 Simple regression results for annual linear extension rate, Sr/Ca and SST 1985-2010

Site	Sr/Ca vs. Extension (Annual)				Extension vs. SST (Annual)			
	R ²	P-value	Slope	Intercept	R ²	P-value	Slope	Intercept
Agat1-1	0.017	0.5381	0.0000649	0.009	0.001	0.8570	0.024	0.686
Apra2-1	0.062	0.2319	-0.0000991	0.009	0.013	0.5940	0.086	-0.942
Asan1-1	0.179	0.0349	0.0003809	0.009	0.280	0.0065	-0.274	8.810
Asan2-1	0.056	0.2551	-0.0001221	0.009	0.005	0.7328	-0.033	2.169

Table 3.9 Simple regression results for annual calcification rate, Sr/Ca and SST 1985-2010

Site	Sr/Ca vs. Calcification (Annual)				Calcification vs. SST (Annual)			
	R ²	P-value	Slope	Intercept	R ²	P-value	Slope	Intercept
Agat1-1	0.049	0.2858	0.0001207	0.009	0.018	0.5236	-0.078	3.775
Apra2-1	0.048	0.2935	-0.0000809	0.009	0.007	0.6986	0.068	-0.206
Asan1-1	0.054	0.2876	0.0001879	0.009	0.178	0.0452	-0.237	7.912
Asan2-1	0.023	0.4735	-0.0000529	0.009	0.002	0.8296	-0.030	2.422

The inclusion of skeletal density in the Sr/Ca-SST regression analysis for the annual datasets significantly improved the calibration for Asan1-1, raising the R^2 value from 0.489 to 0.663 (Table 3.10). However, as before, no significant improvement was achieved for the other three cores. Neither including extension rate nor calcification rate in the regression significantly improved the calibration equation for any of the four cores (Table 3.11 and 3.12).

Table 3.10 Multiple regression results for annual Sr/Ca, skeletal density and SST 1985-2010. * indicates significant improvement over original Sr/Ca-SST equation.

Sr/Ca vs. SST and Density (Annual)						
Site	Original R^2	R^2	P-value	Partial Slope SST	Partial Slope Density	Intercept
Agat1-1	0.062	0.067	0.4638	-0.0000682	0.0001257	0.011
Apra2-1	0.016	0.057	0.5267	-0.0000279	0.0010000	0.009
Asan1-1	0.489	0.663*	<0.0001	-0.0002833	-0.0010000	0.018
Asan2-1	0.022	0.032	0.7009	0.0000334	0.0000952	0.008

Table 3.11 Multiple regression results for annual Sr/Ca, linear extension rate and SST 1985-2010

Sr/Ca vs. SST and Extension (Annual)						
Site	Original R^2	R^2	P-value	Partial Slope SST	Partial Slope Exten.	Intercept
Agat1-1	0.062	0.079	0.4048	-0.0000795	0.0000697	0.011
Apra2-1	0.016	0.071	0.4448	-0.0000301	-0.0000947	0.010
Asan1-1	0.489	0.493	0.0006	-0.0003071	0.0000672	0.018
Asan2-1	0.022	0.073	0.4348	0.0000309	-0.0001173	0.008

Table 3.12 Multiple regression results for annual Sr/Ca, calcification and SST 1985-2010

Sr/Ca vs. SST and Calcification (Annual)						
Site	Original R ²	R ²	P-value	Partial Slope SST	Partial Slope Calc.	Intercept
Agat1-1	0.062	0.096	0.3284	0.0000001	0.0001111	0.011
Apra2-1	0.016	0.059	0.5104	-0.0000329	-0.0000776	0.010
Asan1-1	0.489	0.583	0.0002	-0.0003657	-0.0000864	0.020
Asan2-1	0.022	0.042	0.6218	0.0000332	-0.0000506	0.008

Other Metal Ratios

Monthly U/Ca and Mg/Ca values were significantly correlated with Sr/Ca in all four cores (Table 3.13). In Apra2-1 and Asan2-1 B/Ca was significantly negatively correlated with Sr/Ca. These relationships suggest that Sr, U, Mg and perhaps B ion incorporation are driven by similar factors. Ba/Ca was poorly correlated with the other metals in all cores except Asan1-1, where it was significantly positively correlated with Sr/Ca.

Table 3.13 Correlation coefficients (R) for monthly metal/Ca ratios and Sr/Ca. * indicates $p < 0.0001$.**

Core	Metal/Ca Ratio	R with Sr/Ca
Apra2-1	B/Ca	-0.342 ***
	Mg/Ca	-0.331 ***
	Ba/Ca	0.065
	U/Ca	0.500 ***
Agat1-1	B/Ca	0.020
	Mg/Ca	-0.574 ***
	Ba/Ca	-0.066
	U/Ca	0.744 ***
Asan1-1	B/Ca	-0.106
	Mg/Ca	-0.371 ***
	Ba/Ca	0.234 ***
	U/Ca	0.592 ***
Asan2-1	B/Ca	-0.391 ***
	Mg/Ca	-0.450 ***
	Ba/Ca	-0.068
	U/Ca	0.750 ***

Empirical Orthogonal Function (EOF) analysis further emphasized this relationship between the metal/Ca ratios. The first EOF, explaining about 40% of the variation in metal/Ca ratios, was dominated by Sr/Ca, U/Ca, and Mg/Ca in all four cores. The second EOF was dominated by Ba/Ca for all four cores, explaining about 20% of the overall variation (Appendix D).

Of the metal ratios Sr/Ca showed the strongest relationship with monthly SST for Asan1-1 and Asan2-1. Ba/Ca for Agat1-1 and Mg/Ca for Apra2-1 showed the strongest relationships with monthly SST, however, R^2 values for both were low. Monthly skeletal density related best with U/Ca in Asan1-1, Asan2-1, and Agat1-1 and with Ba/Ca in Apra2-1. EOF1 was significantly related to monthly skeletal density for Agat1-1, Asan1-1 and Asan2-1 and to monthly SST for Asan1-1 and Asan2-1 (Table 3.14).

Table 3.14 Simple regression results for monthly metal/Ca ratios, SST and skeletal density 1985-2010. * indicates $p < 0.05$, ** indicates $p < 0.001$, * indicates $p < 0.0001$**

Core	Metal/Ca Ratio	R ² Density	R ² SST
Agat1-1	Ba/Ca	0.010	0.022 *
	B/Ca	0.004	0.007
	Mg/Ca	0.017 *	0.003
	Sr/Ca	0.026 **	0.003
	U/Ca	0.037 ***	0.000
	EOF1	0.024 **	0.003
Apra2-1	Ba/Ca	0.020 *	0.031 **
	B/Ca	0.007	0.017 *
	Mg/Ca	0.005	0.079 ***
	Sr/Ca	0.002	0.001
	U/Ca	0.013	0.002
	EOF1	0.000	0.040 **
Asan1-1	Ba/Ca	0.003	0.034 **
	B/Ca	0.058 ***	0.051 ***
	Mg/Ca	0.130 ***	0.163 ***
	Sr/Ca	0.223 ***	0.404 ***
	U/Ca	0.226 ***	0.278 ***
	EOF1	0.239 ***	0.361 ***
Asan2-1	Ba/Ca	0.016 *	0.000
	B/Ca	0.023 **	0.033 **
	Mg/Ca	0.012	0.081 ***
	Sr/Ca	0.039 ***	0.251 ***
	U/Ca	0.078 ***	0.223 ***
	EOF1	0.045 **	0.240 ***

Annual data showed a different story. Many fewer significant correlations were found between the metal/Ca ratios, SST, and the three annual growth parameters (Table 3.15). U/Ca related best to annual SST for Agat1-1 and Asan1-1. Mg/Ca for Apra2-1 and B/Ca for Asan2-1 related best. U/Ca showed the strongest relationship with annual skeletal density for Asan1-1 and B/Ca showed the strongest for Asan2-1. No significant relationships between metal/Ca ratios and density were found for Agat1-1 and Apra2-1. Likewise, no significant relationships were found between metal/Ca ratios and annual

linear extension rates for Agat1-1, Apra2-1, and Asan2-1, and no significant relationships were found with calcification for any metal/Ca ratio in any of the cores. Sr/Ca was the only metal/Ca ratio to show a significant relationship to linear extension rate for Asan1-1.

Table 3.15 Regression coefficients (R^2) for annual metal/Ca ratios, SST, skeletal density, linear extension rate, and calcification. * indicates $p < 0.05$, ** indicates $p < 0.001$, * indicates $p < 0.0001$.**

Core	Metal/Ca Ratio	SST	Density	Extension	Calcification
Agat1-1	Ba/Ca	0.027	0.001	0.003	0.007
	B/Ca	0.174 *	0.010	0.060	0.062
	Mg/Ca	0.159 *	0.046	0.053	0.025
	Sr/Ca	0.059	0.027	0.017	0.049
	U/Ca	0.216 *	0.081	0.013	0.088
Apra2-1	Ba/Ca	0.014	0.000	0.015	0.018
	B/Ca	0.041	0.004	0.054	0.069
	Mg/Ca	0.324 **	0.006	0.085	0.085
	Sr/Ca	0.016	0.048	0.062	0.048
	U/Ca	0.013	0.141	0.006	0.026
Asan1-1	Ba/Ca	0.005	0.123	0.040	0.011
	B/Ca	0.123	0.143	0.041	0.004
	Mg/Ca	0.320 **	0.148	0.009	0.000
	Sr/Ca	0.489 ***	0.343 **	0.180 *	0.054
	U/Ca	0.581 ***	0.466 ***	0.124	0.016
Asan2-1	Ba/Ca	0.021	0.056	0.063	0.011
	B/Ca	0.392 ***	0.158 *	0.001	0.044
	Mg/Ca	0.149	0.000	0.029	0.024
	Sr/Ca	0.022	0.012	0.056	0.022
	U/Ca	0.321 **	0.004	0.012	0.003

Because U/Ca repeatedly corresponded with both SST and growth parameters more strongly and with less variability than Sr/Ca, especially for Asan1-1 and it has been used as an SST proxy before, the growth-dependent SST regression analyses were repeated, substituting U/Ca for Sr/Ca. The calibration equations based off monthly data

were not improved by using U/Ca, although, the regression was significant for Asan1-1. For the annual data, the growth-dependent U/Ca-SST calibration equation for Asan1-1 had an R^2 value of 0.741 which is greater than the 0.663 achieved using the Sr/Ca proxy. The regression was not significant for the other three cores (Table 3.16).

Table 3.16 Multiple regression results for U/Ca (Monthly and Annual), SST and skeletal density 1985-2010. * indicates a significant improvement over the Sr/Ca analysis.

U/Ca vs. SST and Density (Monthly)						
Core	Sr/Ca R^2	R^2	P-Value	Partial Slope SST	Partial Slope Den	Intercept
Agat1-1	0.026	0.043	0.0014	-0.000000007	0.000000150	0.00000147
Apra2-1	0.004	0.019	0.0621	-0.000000007	0.000000143	0.00000147
Asan1-1	0.454	0.336	<0.0001	-0.000000059	-0.000000241	0.00000338
Asan2-1	0.253	0.227	<0.0001	-0.000000044	-0.000000057	0.00000260
U/Ca vs. SST and Density (Annual)						
Core	Sr/Ca R^2	R^2	P-Value	Partial Slope SST	Partial Slope Den	Intercept
Agat1-1	0.067	0.237	0.0513	-0.000000087	0.000000132	0.00000379
Apra2-1	0.057	0.143	0.1824	-0.000000011	0.000000652	0.00000102
Asan1-1	0.663	0.741*	<0.0001	-0.000000232	-0.000000755	0.00000896
Asan2-1	0.032	0.331	0.0120	-0.000000131	0.000000088	0.00000491

Other Environmental Influences

Clear annual periodicity is apparent in all of the environmental parameters except for the ENSO (MEI) index which had a more complex structure (Fig 3.11-12). All environmental parameters were significantly correlated with SST. Mean sea level and rainfall were positively related and all others were negatively related (Table 3.17). Wave height was the most tightly correlated environmental factor to SST with a correlation coefficient of -0.768, but even that displayed enough unique variability separate of SST

to warrant exploration of its effects on the Sr/Ca ratios and growth parameters. Peak period and average period were closely correlated with one another ($R=0.846$), so peak period was eliminated from further analysis.

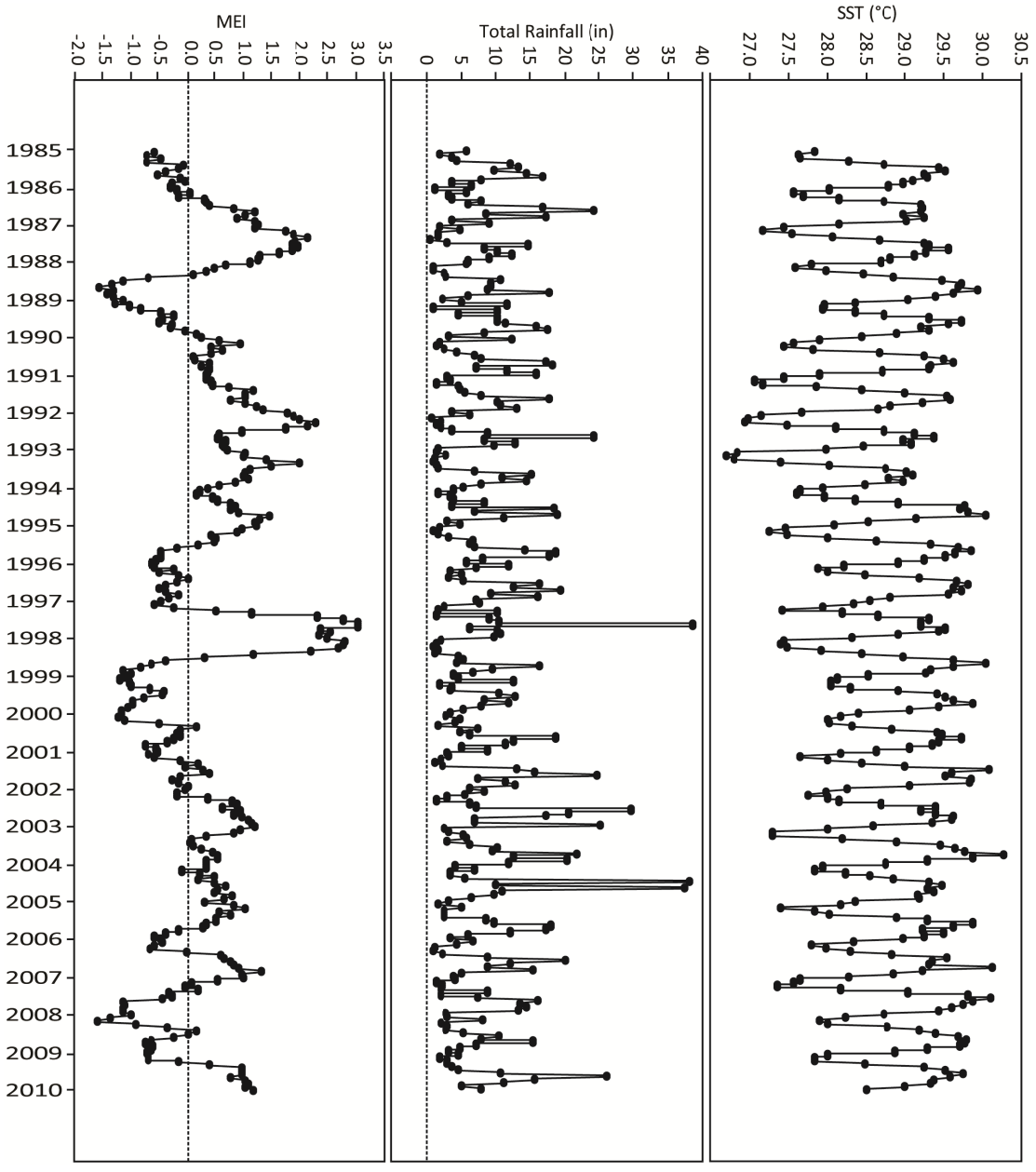


Figure 3.11 Environmental time series for SST, total rainfall, and MEI 1985-2010

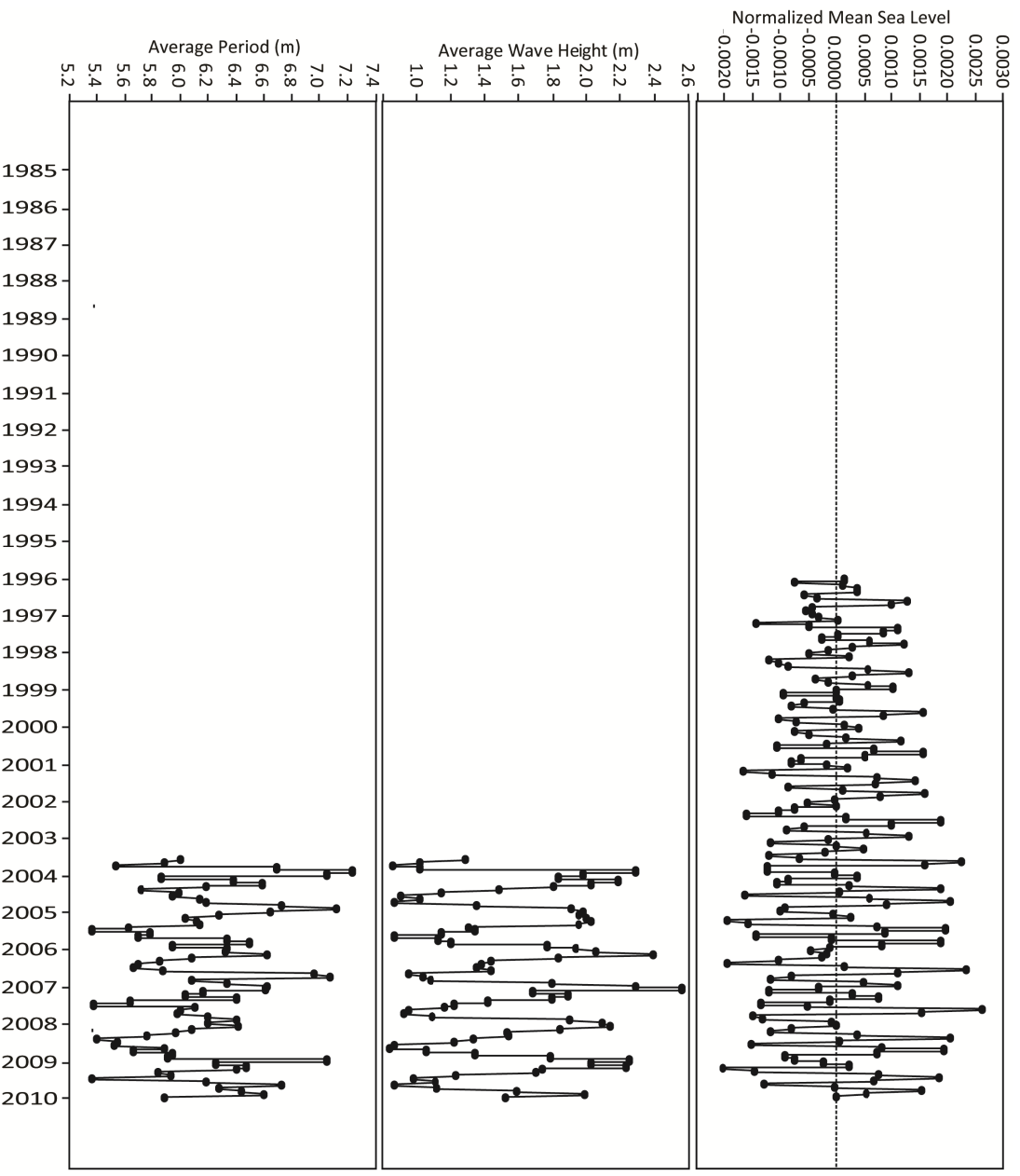


Figure 3.12 Environmental time series for mean sea level, wave height and average period 1985-2010

Table 3.17 Correlation coefficients between SST and the other environmental parameters

Parameter	R with SST	P-Value
Avg. Period	-0.189	0.0008
MEI	-0.194	<0.0001
Mean Sea Level	0.330	<0.0001
Peak Period	-0.208	0.0002
Rainfall	0.556	<0.0001
Wave Height	-0.768	<0.0001

Monthly Sr/Ca ratios for each core were regressed against each environmental parameter individually (Table 3.18). Sr/Ca for Apra2-1 was not significantly correlated with any environmental parameter. Rainfall was significantly correlated with Sr/Ca for Agat1-1, Asan1-1, and Asan2-1. Average wave height and mean sea level were significantly correlated with Sr/Ca for Asan1-1 and Asan2-1. MEI was significantly correlated with Sr/Ca only in Asan1-1. Average period was not significantly correlated for any core.

Table 3.18 Simple regression results between monthly Sr/Ca and environmental parameters 1985-2010

Agat1-1	R ²	P-Value	Slope	Intercept
Avg. Period	0.030	0.1297	0.00004116	0.009
MEI	0.002	0.4661	0.00000481	0.009
Mean Sea Level	<0.000	0.8398	-0.002	0.009
Rainfall	0.017	0.0224	0.00000220	0.009
SST	0.003	0.3264	0.00000757	0.009
Wave Height	0.003	0.6218	0.00001286	0.009

Apra2-1	R ²	P-Value	Slope	Intercept
Avg. Period	0.001	0.7927	0.00000789	0.009
MEI	0.002	0.4132	0.00000522	0.009
Mean Sea Level	0.005	0.3531	0.008	0.009
Rainfall	0.001	0.5118	-0.0000006	0.009
SST	0.001	0.6211	-0.0000037	0.009
Wave Height	0.007	0.4513	0.00002151	0.009

Asan1-1	R ²	P-Value	Slope	Intercept
Avg. Period	0.012	0.3311	0.00003580	0.009
MEI	0.024	0.0074	0.00002449	0.009
Mean Sea Level	0.052	0.0029	-0.030	0.009
Rainfall	0.166	<0.0001	-0.0000095	0.009
SST	0.404	<0.0001	-0.0001179	0.013
Wave Height	0.374	<0.0001	0.0001872	0.009

Asan2-1	R ²	P-Value	Slope	Intercept
Avg. Period	<0.000	0.8660	-0.00000417	0.009
MEI	0.002	0.4781	0.00000476	0.009
MSL	0.029	0.0267	-0.019	0.009
Rainfall	0.109	<0.0001	-0.0000059	0.009
SST	0.251	<0.0001	-0.0000679	0.011
Wave Height	0.195	<0.0001	0.00009052	0.009

Stepwise regression analyses were performed for each core between monthly Sr/Ca and the suite of environmental parameters to determine which were the most important drivers of Sr/Ca incorporation (Table 3.19). For Agat1-1 and Apra2-1, no

environmental parameters was significantly correlated enough to be included in the model. For Asan1-1, SST, MEI and Rainfall remained in the model, together explaining 60% of the Sr/Ca variability. For Asan2-1, SST and Rainfall were the best explanatory variables, predicting 34% of the Sr/Ca variability when combined.

Table 3.19 Stepwise regression results for monthly Sr/Ca vs. six environmental parameters (SST, rainfall, MEI, wave height, mean sea level, average period)

Sr/Ca vs. Environmental Parameters					
Site	R ²	P-Value	Factors In-Model	Partial Slope	Intercept
Agat1-1	-	-	None	-	-
Apra2-1	-	-	None	-	-
Asan1-1	0.606	<0.0001	SST MEI Rainfall	-0.0001060 -0.0000639 -0.0000037	0.012
Asan2-1	0.335	<0.0001	SST Rainfall	-0.0000543 -0.0000014	0.011

Annually averaged Sr/Ca and environmental parameters were compared individually using regression analysis (Table 3.20). Average wave height and average period were not compared because the limited number of years available in the period of interest (2003-2010) was not enough for statistical analysis of annual trends. Only rainfall was significantly correlated with annual Sr/Ca in Asan1-1. No other environmental parameter other than SST was significantly correlated with annual Sr/Ca in any of the cores. Stepwise regression between annual Sr/Ca and the four environmental parameters for Agat1-1, Apra2-1 and Asan2-1 returned empty models. Rainfall remained the only parameter in the Asan1-1 stepwise model reporting an R² of 0.285.

Table 3.20 Simple regression results between annual Sr/Ca and environmental parameters 1985-2010

Agat1-1	R ²	P-Value	Slope	Intercept
MEI	0.031	0.4022	0.00001878	0.009
Mean Sea Level	0.001	0.9026	0.037	0.009
Rainfall	0.116	0.0957	0.00001547	0.009
SST	0.060	0.2391	-0.0000778	0.011

Apra2-1	R ²	P-Value	Slope	Intercept
MEI	0.039	0.3432	0.00002042	0.009
Mean Sea Level	0.006	0.7901	-0.076	0.009
Rainfall	0.147	0.0582	-0.0000168	0.009
SST	0.016	0.5530	-0.0000382	0.010

Asan1-1	R ²	P-Value	Slope	Intercept
MEI	0.110	0.1048	0.00005208	0.009
Mean Sea Level	0.007	0.7804	0.066	0.009
Rainfall	0.189	0.0301	-0.0000288	0.009
SST	0.489	0.0001	-0.0003255	0.018

Asan2-1	R ²	P-Value	Slope	Intercept
MEI	0.039	0.3452	0.00001568	0.009
Mean Sea Level	0.053	0.4285	0.157	0.009
Rainfall	0.005	0.7256	0.00000249	0.009
SST	0.022	0.4830	0.00003470	0.008

Monthly skeletal density measurements were regressed against environmental parameters individually (Table 3.21). Rainfall was significantly correlated with density in all four cores. Density was also significantly correlated with mean sea level, average period and wave height for Agat1-1. For Apra2-1 and Asan2-1 MEI was significantly correlated, and for Asan1-1 and Asan2-1, wave height was significantly correlated.

Table 3.21 Simple regression results between monthly skeletal density and environmental parameters 1985-2010

Agat1-1	R ²	P-Value	Slope	Intercept
MEI	0.002	0.4408	-0.005	1.108
Mean Sea Level	0.068	0.0006	22.766	1.076
Rainfall	0.034	0.0013	0.003	1.084
SST	0.083	<0.0001	0.036	0.080
Avg. Period	0.053	0.0428	-0.048	1.360
Wave Height	0.133	0.0010	-0.073	1.176

Apra2-1	R ²	P-Value	Slope	Intercept
MEI	0.020	0.0143	0.011	1.133
Mean Sea Level	0.058	0.4590	4.489	1.137
Rainfall	0.025	0.0056	0.002	1.122
SST	0.086	<0.0001	0.026	0.394
Avg. Period	0.003	0.6619	0.009	1.090
Wave Height	0.016	0.2760	-0.022	1.180

Asan1-1	R ²	P-Value	Slope	Intercept
MEI	0.007	0.1631	0.011	1.181
Mean Sea Level	0.017	0.0917	15.853	1.216
Rainfall	0.103	<0.0001	0.006	1.133
SST	0.297	<0.0001	0.087	-1.304
Avg. Period	<0.000	0.9499	0.002	1.219
Wave Height	0.189	<0.0001	-0.114	1.405

Asan2-1	R ²	P-Value	Slope	Intercept
MEI	0.022	0.0097	-0.016	1.279
Mean Sea Level	0.009	0.2198	9.339	1.281
Rainfall	0.093	<0.0001	0.005	1.236
SST	0.223	<0.0001	0.060	-0.452
Avg. Period	<0.000	0.9298	0.002	1.283
Wave Height	0.062	0.0273	-0.048	1.369

Stepwise regression tests between monthly density measurements and the suite of environmental parameters revealed the dominant effectors of density to be SST and MEI (Table 3.22). SST and MEI both remained in the model for Agat1-1 and Asan2-1, whereas MEI alone and SST alone remain for Asan1-1 and Apra2-1, respectively.

Table 3.22 Stepwise regression results between monthly density and environmental parameters 1985-2010

Mean Density vs. Environmental Parameters					
Site	R ²	P-Value	Factors In-Model	Partial Slope	Intercept
Agat1-1	0.209	0.0001	SST	0.046	-0.280
			MEI	0.030	
Apra2-1	0.108	0.0033	MEI	0.038	1.143
Asan1-1	0.409	<0.0001	SST	0.103	-1.1747
Asan2-1	0.131	0.0052	SST	0.032	0.373
			MEI	0.028	

Annual density and the environmental parameters were also compared individually (Table 3.23). Mean sea level was the parameter most strongly correlated with annual density for Agat1-1, and other than SST and annual density for Asan1-1, no other parameter significantly correlated with density for any of the remaining three cores. Stepwise regression relayed a slightly different impression (Table 3.24). MEI and mean sea level remain in the Agat1-1 annual density model explaining 52% of the variability in density. No parameters were strongly correlated enough with annual density to remain in the models for Apra2-1 and Asan1-1. MEI and SST remain in the model for Asan2-1 explaining 65% of the variability in annual density.

Table 3.23 Simple regression results between annual density and environmental parameters 1985-2010

Agat1-1	R ²	P-Value	Slope	Intercept
MEI	0.029	0.4174	-0.013	1.110
Mean Sea Level	0.304	0.0411	260.419	1.074
Rainfall	0.016	0.5519	-0.004	1.140
SST	0.106	0.1127	-0.077	3.311

Apra2-1	R ²	P-Value	Slope	Intercept
MEI	0.156	0.0506	0.016	1.132
Mean Sea Level	0.138	0.1916	149.318	1.136
Rainfall	0.005	0.7354	0.001	1.127
SST	0.027	0.4349	-0.019	1.694

Asan1-1	R ²	P-Value	Slope	Intercept
MEI	0.003	0.7988	-0.005	1.186
Mean Sea Level	0.153	0.6026	-57.491	1.217
Rainfall	0.002	0.8469	0.001	1.173
SST	0.171	0.0496	0.098	-1.643

Asan2-1	R ²	P-Value	Slope	Intercept
MEI	0.036	0.3619	0.016	1.260
Mean Sea Level	0.041	0.4891	107.330	1.282
Rainfall	0.003	0.3129	0.008	1.204
SST	0.003	0.7906	0.014	0.861

Table 3.24 Stepwise regression results between annual skeletal density and environmental parameters 1985-2010

Annual Density vs. Environmental Parameters					
Site	R ²	P-Value	Factors In-Model	Partial Slope	Intercept
Agat1-1	0.524	0.0168	MEI Mean Sea Level	-0.030 315.120	1.078
Apra2-1	-	-	None	-	-
Asan1-1	-	-	None	-	-
Asan2-1	0.648	0.0032	SST MEI	0.444 0.092	-11.538

Linear extension rate and calcification rate were also compared to the individual environmental parameters in simple regression tests and to the suite of environmental parameters in a stepwise regression test. Rainfall was significantly related to both linear extension rate and calcification with R^2 values of 0.255 ($p=0.0100$) and 0.291 ($p=0.0079$), respectively. Stepwise regressions, likewise, returned empty models for Agat1-1 and Apra2-1 and only rainfall remained in the Asan1-1 models for both linear extension rate and calcification rate ($R^2 = 0.432$ and 0.377 , respectively).

Results Summary

Tables 3.25, 3.26, and 3.27 provide a summary of the regression analyses discussed above. These analyses showed that Sr/Ca was not well associated with SST, growth parameters, or other environmental parameters in the Agat1-1 and Apra2-1 cores (p -values > 0.05 or R^2 values < 0.25). The Sr/Ca record found in Asan2-1 was moderately related to monthly SST and environmental parameters (p -values < 0.05 with R^2 values > 0.5). Sr/Ca was moderately related to monthly SST, annual SST, and annual density measurements in Asan1-1. Additionally, Sr/Ca-SST regressions that included annual density and calcification resulted in $R^2 > 0.5$ for Asan1-1. Monthly density was weakly related with SST and rainfall in the four cores, and annual growth parameters were only related to these individual environmental parameters in Asan1-1. However, taken together environmental parameters explain more than 50% of the variation in annual density for Agat1-1 and Asan2-1. U/Ca was also found to relate significantly to SST in Asan1-1, and the annual U/Ca-SST regression equation with skeletal density gave the highest R^2 value (0.741) of all the regressions discussed in this study.

Table 3.25 Summary of Sr/Ca regression results. All letters represent p-values < 0.05. “X” denotes $R^2 < 0.25$, “S” denotes $0.25 < R^2 < 0.50$, and “G” denotes $R^2 > 0.50$. Blank spaces indicate the results were not statistically significant ($p > 0.05$).

Regression Analysis	Monthly				Annual			
	Agat1-1	Apra2-1	Asan1-1	Asan2-1	Agat1-1	Apra2-1	Asan1-1	Asan2-1
Sr/Ca vs. SST			S	S			S	
Sr/Ca vs. Avg. Period								
Sr/Ca vs. MEI			X					
Sr/Ca vs. MSL			X	X				
Sr/Ca vs. Rainfall	X		X	X			X	
Sr/Ca vs. Wave Height			S	S				
Sr/Ca vs. Env. (Stepwise)			G-SST,MEI,Rain	S-SST,Rain			S-Rainfall	
Sr/Ca vs. Den.	X		X	X			S	
Sr/Ca vs. Ext.							X	
Sr/Ca vs. Calc.								
Sr/Ca vs. SST and Den.	X		S	S			G	
Sr/Ca vs. SST and Ext.							S	
Sr/Ca vs. SST and Calc.							G	

Table 3.26 Summary of coral growth regression results. All letters represent p-values < 0.05. “X” denotes $R^2 < 0.25$, “S” denotes $0.25 < R^2 < 0.50$, and “G” denotes $R^2 > 0.50$. Blank spaces indicate the results were not statistically significant ($p > 0.05$).

	Density (Monthly)				Density (Annual)			
Regression Analysis	Agat1-1	Apra2-1	Asan1-1	Asan2-1	Agat1-1	Apra2-1	Asan1-1	Asan2-1
Growth vs. Sr/Ca	X		X	X			S	
Growth vs. SST	X	X	S	X			X	
Sr/Ca vs. SST and Growth	X		S	S			G	
Growth vs. Avg. Period								
Growth vs. MEI		X		X				
Growth vs. MSL	X				S			
Growth vs. Rainfall	X	X	X	X				
Growth vs. Wave Height	X		X	X				
Growth vs. Env. (Stepwise)	X-SST,MEI	X-MEI	S-SST	X-SST,MEI	G-MEI,MSL			G-SST,MEI

	Extension (Annual)				Calcification (Annual)			
Regression Analysis	Agat1-1	Apra2-1	Asan1-1	Asan2-1	Agat1-1	Apra2-1	Asan1-1	Asan2-1
Growth vs. Sr/Ca			X					
Growth vs. SST			S				X	
Sr/Ca vs. SST and Growth			S				G	
Growth vs. Avg. Period								
Growth vs. MEI								
Growth vs. MSL								
Growth vs. Rainfall			S				S	
Growth vs. Wave Height								
Growth vs. Env. (Stepwise)			S-Rainfall				S-Rainfall	

Table 3.27 Summary of U/Ca regression results. All letters represent p-values < 0.05. “X” denotes $R^2 < 0.25$, “S” denotes $0.25 < R^2 < 0.50$, and “G” denotes $R^2 > 0.50$. Blank spaces indicate the results were not statistically significant ($p > 0.05$).

Regression Analysis	Monthly				Annual			
	Agat1-1	Apra2-1	Asan1-1	Asan2-1	Agat1-1	Apra2-1	Asan1-1	Asan2-1
U/Ca vs. SST			S	X	S		G	S
U/Ca vs. Density	X		X	X			S	
U/Ca vs. Extension								
U/Ca vs. Calcification								
U/Ca vs. SST and Den.	X		S	X			G	S
U/Ca vs. SST and Ext.								
U/Ca vs. SST and Calc.								

Chapter 4: Discussion

Four coral cores were analyzed from three reef sites on Guam to further understand the Sr/Ca-SST relationship and how it may be affected by coral growth, in an effort to improve our ability to use Sr/Ca as a proxy to reconstruct sea surface temperature for Guam. The relationship between Sr/Ca and SST temperature proved to be weak at best and surprisingly variable between cores even on small spatial scales. Growth calibration was unsuccessful at explaining the weakness in the Sr/Ca-SST relationship. Rainfall and the Multivariate ENSO Index (MEI) present some possible explanations for Sr/Ca variation, but, in general, analyses presented here provided more questions than answers. These facts leave the author to consider whether or not Sr/Ca measured from coral cores can be appropriately used to reconstruct SST for Guam.

Sr/Ca-SST relationship

The primary goals of this study was to determine how well Sr/Ca corresponded with SST in the four coral cores from Guam, and, as a result, how accurately historical SST could be reconstructed considering only the Sr/Ca proxy. No significant relationship was found between Sr/Ca and SST for two of the four cores analyzed (Agat1-1 and Apra2-1). SST explained 40% and 25% of the variation in monthly Sr/Ca in Asan1-1 and Asan2-1, respectively, and 49% of the variation in annual Sr/Ca for Asan1-1. (The Sr/Ca-SST relationship for annual data was insignificant for Asan2-1.) This result is surprising, given the great body of literature supporting a strong relationship between Sr/Ca and SST, often with R^2 values of 0.90 or higher (reviewed by Corregge 2006), but it is not completely unprecedented.

Through an extensive literature search, three studies were found to have similarly weak Sr/Ca-SST calibration results. Alibert and Kinsley (2008) collected three coral cores off Papua New Guinea. Sr/Ca from two cores proved too difficult to match to SST record, and the third showed an unusually steep relationship with SST. A coral core analyzed from the Solomon Islands (Liu et al. 2012) exhibited a Sr/Ca-SST relationship with an R^2 of only 0.39, even after correcting for a decade long drift. Additionally, Correge (2006) reports an unpublished R^2 of 0.42 for a *Porites* Sr/Ca record from Fiji. Notably, all three of these studies, as well as the current study, occurred in the area defined as the Western Pacific Warm Pool (Cravatte et al. 2009).

The Western Pacific Warm Pool (WPWP) is the warmest region of the Pacific Ocean, with average SST warmer than 28-29°C (Cravatte et al. 2009). Throughout the time period studied, SST around Guam experienced an average monthly temperature range of less than four degrees and average annual temperature range of less than one degree Celsius. This range is smaller than those of the regions of all of the studies reviewed by Correge (2006). Perhaps analyzing Sr/Ca against such a narrow temperature range, contributed to the weaknesses found in the SST relationship. Evidence supporting that the poor Sr/Ca-SST relationship may stem from the narrow temperature range was found with further inspection of the annual Sr/Ca-SST relationships. During the period between 1989 and 1994 when temperatures spanned a wider than typical range for a 6-year period (0.80°C, compared with median range of 0.38°C), annual Sr/Ca and SST were strongly related for Asan1-1 and Apra2-1.

In addition to the weaknesses in the relationships, the significant monthly Sr/Ca-SST calibration equations differed from those reported in literature. The equation for

Asan2-1 has a higher intercept and steeper slope than the average calibration equation for *Porites* studies reported by Correge (2006) and that of Bell et al. (2011a), but is within the range of reported equations. The slope for the Asan1-1 equation, however, was nearly twice as steep and with a higher intercept than that reported in any of the reviewed equations (Correge 2006). The only equation with a slope as steep found in literature was from the core studied by Alibert and Kinsley (2008) in Papua New Guinea for which the slope was even twice that of Asan1-1.

It is clear from this analysis that SST is not the only controlling factor of strontium incorporation in the Guam cores and may not be even a dominant driver in some of the corals studied. Despite the fact that the seasonality in SST at all three locations is similar, the distinctness of Sr/Ca records of the four cores is striking. Variation Sr/Ca measured in the Agat1-1 and Apra2-1 cores does not show an annual structure, and there is even little congruence between these two records. Furthermore, the Sr/Ca record from a second core from Agat (Agat2-1, data not shown) collected just a few meters from Agat1-1 showed another completely distinct pattern. Asan1-1 and Asan2-1, collected less than 500m from one another also show differing responses to SST, despite their physical proximity. Although both Sr/Ca records collected from Asan showed annual Sr/Ca patterns and significant relationships to monthly SST, Sr/Ca for Asan1-1 appeared to respond to SST changes on average annual scale, whereas the Asan2-1 record did not.

Given the understanding that Sr/Ca in coral cores is typically closely correlated with SST, and that the relationship is driven by SST-modified incorporation of Sr/Ca from functionally stable seawater Sr/Ca concentrations, as discussed in Chapter 1, the

weaknesses in the Sr/Ca-SST relationship found here can logically be caused only by two things. Either 1.) the SST dependence of the strontium incorporation pathways are modified in these corals, or 2.) the seawater Sr/Ca concentrations are less constant than typical at these locations. Studying either of these potential causes directly is outside the scope of this study. However, the growth-dependent Sr/Ca-SST calibration and a brief analysis of the relationship between Sr/Ca and the available environmental parameters below gives insight into these two possibilities.

Growth-dependent Sr/Ca-SST Model

Strontium incorporation is linked to skeleton formation and mediated by at least two separate mechanisms (passive and active transport) which could be affected by many localized environmental conditions. Therefore, variations in coral growth were the primary putative cause of the observed coral-to-coral discrepancies in the Sr/Ca record and weaknesses in the Sr/Ca-SST relationship observed in this study. However, exploration of how coral growth was related to SST and Sr/Ca revealed little evidence to support that coral growth was a primary cause of either. Skeletal density, linear extension rate, and calcification rates were found to be only weakly related to SST and Sr/Ca, and these growth parameters explained little of the differences in Sr/Ca records between corals.

SST was related to skeletal density in the cores, but large amounts of variation in growth parameters were unexplained by SST. Seasonal density bands were visually obvious in Asan1-1 and Asan2-1 and less pronounced, but present, in Agat1-1 and Apra2-1. Monthly skeletal density was positively and significantly related to SST in all four cores, but 70 to 92% of variation in monthly skeletal density could not be explained

by SST. Furthermore, annual skeletal density, linear extension rate, and calcifications rates were only significantly related to SST in Asan1-1 with 72 to 83% of the variation in those parameters left unexplained by SST. This result is unexpected.

A positive relationship between coral growth and SST is well supported in the literature. Among other studies, Weber et al. (1975) found that linear extension rate was positively related to SST in a study of 47 genera and subgenera over 31 localities in the Indo-Pacific and Caribbean, and a study of 245 massive *Porites* from the Great Barrier Reef showed that linear extension rate and calcification rate increased with increasing SST (Lough and Barnes 2000). Nonetheless, three of the four cores analyzed here showed no significant relationship between either linear extension rate or calcification rate and SST. Perhaps this is again attributable to the narrow temperature range experienced on Guam's reefs. Though such an effect is not reported in coral core literature, annual growth increments in marine fish otoliths, also typically caused by seasonal temperature fluctuations, have been reported to decrease in clarity with decreasing temperature range. An annual SST range of 4-5°C has been shown to be necessary to produce discernible increments in otoliths for aging tropical fish (Meekan et al. 1999; Caldow and Wellington 2003).

The unexplained variation in coral growth included great dissimilarity in monthly and annual scale growth measurements from core to core which was expected, but the correspondence between these measurements and Sr/Ca records was less than anticipated. On the other hand, if SST was not a dominant controlling factor of coral growth as indicated by the regression results discussed in the preceding paragraph, it is unreasonable to expect a significant relationship between Sr/Ca and SST since strontium

incorporation is linked to skeleton formation (Cohen et al. 2001, Cohen et al. 2002, Ferrier-Pages et al. 2002, Cohen and McConnaughey 2003). Here, monthly skeletal density was related to Sr/Ca for all cores except Apra2-1, but skeletal density only explained two and four percent of variation in Sr/Ca for Agat1-1 and Asan2-1, respectively. Annual skeletal density and linear extension rates were only significantly related to Sr/Ca in Asan1-1. Calcification rates were not significantly related to Sr/Ca for any core.

Consequently, the Sr/Ca-SST calibration equation was improved by considering these growth parameters only for Asan1-1. The Asan1-1 equation was improved for both monthly and annual datasets when skeletal density was added as an independent variable to the regression analysis. The new regression equations for Asan1-1 monthly and annual data have R^2 values of 0.454 and 0.663, respectively. The consideration of linear extension rate and calcification rates failed to improve the Asan1-1 regression equation, and no growth parameter improved the regression equations of Agat1-1, Apra2-1, or Asan2-1.

A few researchers have attempted similar growth-dependent Sr/Ca-SST calibrations with positive results. Goodkin et al. (2005) found that linear extension rate could be used to improve an annually averaged Sr/Ca-SST calibration from an R^2 of 0.21 to 0.68 (the monthly Sr/Ca-SST calibration had an R^2 of 0.86). Following that study, Goodkin et al. (2007) developed a multi-coral growth-dependent model, which successfully improved the accuracy of the calibration for three corals. Here growth-calibration was unsuccessful with three of the four cores, and only skeletal density could be used to improve the regression for the fourth core. Therefore, neither SST, growth

parameters, nor a combination of the two could explain the majority of the Sr/Ca records uncovered in this study.

The lack of correspondence between growth parameters and Sr/Ca and the failure of growth-calibration to improve Sr/Ca-SST regressions for three of the four cores (Agat1-1, Apra2-1 and Asan2-1) could have been produced by a few possible scenarios. First, variation in monthly or annual growth in those corals may not have been great enough to produce significant changes in Sr/Ca in those cores (i.e. the corals grew at such a constant rate that the effect of growth on Sr/Ca is undetectable). If that was the case, one would expect that variation in coral growth was greater in the fourth core, Asan1-1, which could be significantly improved by considering skeletal density. Asan1-1 did have the greatest standard deviation for monthly density values, but it did not for any of the annual coral growth parameters. A second explanation is that seawater Sr/Ca was less constant than expected, and the effects of that were greater than the effects of growth. This is discussed further below.

Environmental Parameters

Although the concentration of strontium in surface seawater relative to calcium remains constant across SST gradients, it may be influenced by other environmental parameters, particularly those which influence water body movement and mixing (de Villiers 1999) such as currents, waves, and sea level. This, in turn, may have an effect on the skeletal Sr/Ca record (Sun et al. 2005). Environmental parameters may also influence coral growth, indirectly affecting the Sr/Ca record. Here Sr/Ca and coral growth parameters were regressed against rainfall, the Multivariate El Niño/Southern Oscillation Index (MEI), mean sea level, wave height, and average wave period to search for

confounding factors to the Sr/Ca-SST relationship and coral growth-SST relationships. In addition to SST, rainfall was found to be an important driving factor for monthly Sr/Ca at the Asan sites. For Asan1-1, MEI was also an important driver of monthly Sr/Ca and rainfall was an important driver for annual Sr/Ca. The most prominent driver of skeletal density on both monthly and annual scales was MEI, and rainfall was a prominent driver of linear extension rate and calcification for Asan1-1.

Correspondence between Sr/Ca and rainfall for the Asan sites, which are located in close proximity to the Asan River, suggests that river runoff is affecting Sr/Ca in the cores. The effect of runoff is likely the result of the alteration of seawater Sr/Ca values. Although Sr/Ca is generally independent of salinity in the open ocean (Correge 2006), a measurable gradient in Sr/Ca concentrations can be found in many estuarine environments, and as a result, Sr/Ca measured in some fish otoliths is read as a life history fingerprint (Secor et al. 2001). Sr/Ca was conserved in seawater despite the presence of river plumes in two reef environments in the Great Barrier Reef and Okinawa, Japan (Alibert et al. 2000; Ramos et al. 2004) leaving skeletal Sr/Ca records relatively clean indicators of SST. On the contrary, runoff appeared to negatively affect the Sr/Ca-SST relationship for a core in the South China Sea, where seawater Sr/Ca was assumed to experience greater than 15% variability based on measurements from a nearby location (Wei et al. 2000).

No seawater Sr/Ca dataset is available for Guam or the Mariana Islands, but it is likely that the greater than 200 cm of rain which falls in Guam each year (Lander and Guard 2000) could have great effects on the seawater composition nearshore. Spatial salinity, temperature, and circulation data are also lacking for Guam's nearshore waters,

but one detailed study in the Asan reef area shows the effects of a heavy rainstorm on the Asan reef area (Storlazzi et al. 2009). A 2-4PSU drop in salinity and 0.5°C drop in temperature resulted from a single heavy rain event in the area near where the Asan1-1 core was collected. Though the salinity and temperature quickly began to recover, these parameters remained lower than normal throughout the entire reef area for nearly one day following the rain event. Furthermore, salinity was consistently lower near the Asan1-1 coring site throughout the rainy, wet season (~32 PSU) compared to the dry season (~34 PSU), and frequent rain events resulted in drops in salinity for brief periods. The salinity range for the 92-day study was 29.19 to 34.48 PSU near the Asan1-1 site. The site of salinity measurements that was closest to where Asan2-1 was collected experienced a slightly narrower range of 30.77 to 34.49 PSU throughout the same period, clearly demonstrating that the effect of river runoff on water quality was present, yet reduced, at this site. Given the fact that river runoff resulting from rainstorms has a measureable influence on salinity in the Asan reef area, it is likely that it has a similar effect on Sr/Ca concentrations if there are significant differences between Sr/Ca concentrations in the two water bodies.

Sr/Ca ratios in freshwater can be either higher or lower than that of seawater depending on the geologic composition of the watershed (Swart et al. 2002). Sr/Ca values measured following a heavy rainstorm in the Asan River near the mouth were on average 3.19 ± 0.24 mmol/mol (Prouty 2013) which is nearly one third the open ocean average of 8.54 ± 0.45 mmol/mol (de Villiers 1999). Low Sr/Ca concentrations from the river could reduce seawater Sr/Ca in the area following rainstorms. If that is the case, the “SST” signal in the Asan1-1 core may be enhanced by increased river discharge. Because Sr/Ca

and SST are inversely related, low Sr/Ca values surrounding the coral would mimic warm temperature Sr/Ca values in the skeletal record. Since Guam's rainy season corresponds with the warmest months of the year, there is potential that the strong "SST" signal in the Asan1-1 core is the cumulative effect of warm temperatures and low seawater Sr/Ca values. Asan2-1 was collected in an area that experiences smaller influence of the Asan River (Storlazzi et al. 2009), so there is less potential for the influence of low Sr/Ca freshwater. This might explain why rainfall was not a significant contributing factor for annual Sr/Ca in Asan2-1 while it was for Asan1-1.

Data on Sr/Ca in the streams which feed the Agat reef area and Apra Harbor are not available, but the soils in southern Guam were found to be rich in strontium and highly contaminated by various other metals (Purdey 2004). This enriched soil could result in high Sr/Ca values in the nearby rivers relative to open ocean concentrations. High Sr/Ca values in runoff might obscure the Sr/Ca record, causing skeletal Sr/Ca not to drop as low as it otherwise would for a given temperature during rain events during the warmer months. Unfortunately, there is also little information on river influence or water circulation in the vicinity of the Agat1-1 and Apra2-1 coring sites.

There are several rivers in Agat, but the specific effects of those on water quality in the reef area near the Agat1-1 coring site are not reported. Storlazzi et al. (2013) found that the water in the Agat reef area tended to be less saline (0.61PSU less) during the wet season compared to the dry season and that turbidity was higher during the same time, though mostly in the northern part of the bay, far from the coring site. This suggests the runoff measurably effect seawater composition in the Agat area. The Agat1-1 core was collected from a patch reef, sheltered by a large rock island (Anae Island) (Stojkovich

1977) which could form an eddy trapping river plumes after rainstorms or the strong currents in the area (Storlazzi et al. 2013) could flush the area quickly. Whatever the case is, circulation dynamics and the influence of runoff appear more complicated at the Agat1-1 coring site than at the Asan sites which is an obvious potential source of differences in the coral records from these sites.

Apra Harbor is a sheltered water body, which has limited mixing with the open ocean. Near surface currents tend to be wind driven, usually moving from the harbor mouth toward the inner harbor due to northeast tradewinds. Deeper water tends to flow the opposite direction, allowing for harbor water to be recycled to the open ocean (Sea Engineering, Inc. 2010). Though the effect on water quality was minimal, evidence of freshwater input was detectable at sites across the harbor from Apra2-1 in a 2008 survey (Sea Engineering, Inc. 2010). Apra2-1 was collected far from any direct river sources and is not expected to experience much runoff from land because the nearest land mass is a long thin peninsula which forms the harbor wall, so there is not much room to accumulate storm water. However, the area likely experiences some effects from the runoff that enters other areas of the harbor since the harbor is not rapidly flushed. Additionally, there is evidence that wind-waves readily resuspend bottom sediments in Apra Harbor. In one case, a 1.5 - 2m wave event raised turbidity levels (on the other side of the harbor from Apra2-1) from a background of <1 NTU to > 20 NTU (Sea Engineering, Inc. 2010). Without testing the Sr/Ca levels in the bottom sediments of Apra Harbor, it is unclear how suspended sediment would affect seawater composition, and possibly as a result, the skeletal Sr/Ca values in the cores. As in Agat, it appears that oceanographic conditions in

Apra Harbor are less straightforward than those in Asan, and that is a likely source of some of the complexities in the skeletal Sr/Ca record.

ENSO events also have the ability to affect seawater concentrations of Sr/Ca because they affect regional water body movements. Ourbak et al. (2006) report a clear record of anomalous sea surface temperatures during the 1990-1994 “long, weak El Niño” in cores from New Caledonia and Wallis Island. This is the expected result since Sr/Ca generally tracks SST, and El Niño events are associated with warm ocean temperatures in that region. However, simultaneously to the temperatures anomalies, El Niño is marked by changes in thermocline depth and rainfall patterns (Wang et al. 2012). Ayliffe et al. (2004) found that a Sr/Ca record extracted from a coral off of New Zealand reflected the lack of pause in the strong northwesterly winds during the 1982-1983, 1987, and 1991-1993 ENSO events which typically resulted in river runoff that affected the Sr/Ca records during the summer months. Similarly, Deng et al. (2013) found that the Pacific Decadal Oscillation (PDO), a comparable phenomenon to ENSO with greater effects in the Northern Pacific Ocean, was not well predicted by Sr/Ca. Rather, runoff events associated with warm PDO events appeared to result in increases of Sr-rich, less saline water, therefore weakening the Sr/Ca and SST relationship.

In the western, off-equatorial Pacific where Guam lies, ENSO events are characterized by cooler SST, decreased thermocline depth, and decreased precipitation (Wang et al. 2012), combined with decreased sea level due to strong westerly winds in the equatorial region (Chowdhury et al. 2007). Cooler temperatures should result in higher Sr/Ca values, but changes in sea level, thermocline depth, and rainfall might result

in altered seawater chemistry which could affect the Sr/Ca values (Wei et al. 2000; Deng et al. 2013).

The cooler temperatures of the 1990-1994 and 1997-1998 ENSO events are clearly represented in the Asan1-1 Sr/Ca record. The effect of these ENSO events on Sr/Ca may have been enhanced at Asan1-1 by the drier weather. Most of the years during these ENSO events had lower than average mean daily rainfall. This would have resulted in less influence of river runoff on the Sr/Ca ratios in the seawater surrounding the Asan1-1 coral. The low Sr/Ca values in the Asan River compared to average open ocean values, discussed above, could affect the Sr/Ca record at this site in the opposite manner. A dry period might result in increased seawater concentration of Sr/Ca compared to the “norm” for this area due to a lack of low Sr/Ca river discharge. Cooler ENSO temperatures are not reflected in the other three Sr/Ca records, and none of these corals are as directly influenced by runoff or the open ocean as Asan1-1. For reasons that were unapparent here, an increase in Sr/Ca in the Asan1-1 in response to the cooler temperatures from the 1987 ENSO is also absent.

In addition to ENSO causing seawater chemistry changes, decreased sea level during ENSO events could have an effect on coral growth as a result of increased photosynthetically active radiation (PAR) available to the zooxanthellae (Cohen and Sohn 2004), which could affect the Sr/Ca record. In the present study, I find that MEI was a significant predicting variable for variation in monthly skeletal density in Agat1-1, Apra2-1, and Asan2-1 and annual skeletal density in Agat1-1 and Asan2-1. However, mean sea level significantly affected annual skeletal density for Agat1-1. Perhaps the

effect of ENSO on coral growth in these cores is responsible for weakening the Sr/Ca-SST relationship.

Rainfall and MEI related to Sr/Ca for Asan1-1 and Asan2-1, and the environmental variables hinted at explanations for the poor Sr/Ca-SST relationships and inconsistency in the four cores. However, the environmental variables tested provided no simple patterns to assist in predicting SST using Sr/Ca records from Guam's corals. Therefore, with our current knowledge, Sr/Ca must be used with caution as an SST proxy for Guam, and more in-depth study of how seawater Sr/Ca, skeletal Sr/Ca, and coral growth parameters are related in Guam's corals is needed.

Other metal/Ca datasets

Some researchers have found in certain cases other metal/Ca ratios are superior predictors of SST over Sr/Ca (Correge 2006, Wei et al. 2000). Consequently, I examined the relationship of Sr/Ca, SST and skeletal density to the other metal/Ca ratios available (B/Ca, Ba/Ca, Mg/Ca, U/Ca). U/Ca, and to a lesser extent Mg/Ca, were found to be significantly correlated with Sr/Ca in all cores. Sr/Ca was still found to be the best predictor of monthly SST in most cases; however, for Asan1-1, U/Ca was the best predictor of annual SST. Furthermore, the highest R^2 value of this study (0.741) was obtained for the annual growth calibrated U/Ca-SST equation for Asan1-1.

U/Ca in the skeleton of massive corals has been tested as a SST proxy in numerous studies (reviewed by Correge 2006). U/Ca records have shown a greater response to SST variations than Sr/Ca (Min et al. 1995), but the incorporation of uranium into the skeleton and its behavior in seawater are not well understood (Correge 2006). While U/Ca often is tightly correlated with Sr/Ca and SST (Correge 2006, Min et al.

1995, Wei et al. 2000), weak associations with SST which vary temporally have also been found, suggesting that the mechanism of incorporation is not a simple function of SST (Correge 2006, Quinn and Sampson 2002).

In the present study, U/Ca was well correlated with Sr/Ca in all four cores, suggesting that the factors driving the U/Ca values are similar to Sr/Ca in these areas. This is particularly interesting for the Agat1-1 and Apra2-1 where the nature of both the Sr/Ca and U/Ca datasets were not the expected annually cyclic patterns seen in Asan1-1 and Asan2-1. Further exploration of this association and that of the other metal/Ca records, while outside the scope of this study, may help to explain the anomalous Sr/Ca records.

Though the Sr/Ca record from Asan1-1 already produced the best association with SST of the four cores, the U/Ca dataset produced an even stronger calibration equation which better predicted SST. With an R^2 value of 0.741, this equation currently has the potential to produce the best reconstruction of SST for Guam for years before the instrumental record. The delta ^{18}O -SST and sea surface salinity reconstruction used to reconstruct ENSO events over a 213 year period reported by Asami et al. (2005) found an R^2 value of 0.48 between delta ^{18}O and SST. The Asan1-1 core is a 111 year record which could potentially expand the SST record about 60 years and verify some of the events in the longer core from Asami et al. (2005). At present, the coral density analysis using the CT scan images has not been completed for the entire core, so the reconstruction cannot yet be performed.

Conclusions and Recommendations

The present analysis of four coral cores revealed great complexities for reconstructing SST for Guam from the skeletal Sr/Ca records. Distinct skeletal Sr/Ca records were found for each of the four cores, and Sr/Ca variation was not reliably explained by SST. Coral growth parameters failed to explain differences in the individual Sr/Ca records, leaving the Sr/Ca-SST calibration equations insignificant for two cores and unique to each of the remaining two cores. There is some evidence that rainfall and ENSO events may have contributed to the complex records, but the variation in the Sr/Ca-SST relationship between cores could not be resolved. Despite the fact that one of the four records presented here and one past record showed promise for SST reconstruction, the inconsistent and complex nature of the skeletal Sr/Ca records extracted from the other cores commands the use of great caution in applying the Sr/Ca-SST thermometry for Guam without a more detailed background study.

At present, the most important, unresolved question is, how does seawater Sr/Ca vary spatially and temporally in Guam's nearshore waters? With this question answered, the validity of the Sr/Ca-SST proxy can be reassessed. A reliable SST reconstruction can only be expected in areas where seawater Sr/Ca is relatively stable. If seawater Sr/Ca is found to be highly variable island-wide, then a less variable elemental parameter which responds to SST in the skeletal record should be chosen as a more appropriate proxy. Future coral-derived proxy analyses should continue give attention to coral growth variations as considerable variation in coral growth parameters between and within cores were found here.

References:

- Alibert, C. and M.T. McCulloch. 1997. Strontium/calcium ratios in modern *Porites* corals from the Great Barrier Reef as a proxy for sea surface temperature: calibration of the thermometer and monitoring of ENSO. *Paleoceanography* 12: 345-363.
- Alibert, C. and L. Kinsley. 2008. A 170-year Sr/Ca and Ba/Ca coral record from the Western Pacific Warm Pool: 1. What can we learn from an unusual coral record? *Journal of Geophysical Research* 113: C04008.
- Allison, N. and A.A. Finch. 2004. High-resolution Sr/Ca records in modern *Porites lobata* corals: Effects of skeletal extension rate and architecture. *Geochemistry Geophysics and Geosystems* 5(5): 1-10.
- Asami, R., T. Yamada, Y. Iryu, T.M. Quinn, C.P. Meyer, and G. Paulay. 2005. Interannual and decadal variability of the western Pacific sea surface condition for the years 1787-2000: Reconstruction based on stable isotope record from a Guam coral. *Journal of Geophysical Research* 110: C05018.
- Ayliffe, L.K., M.I. Bird, M.K. Gagan, P.J. Isdale, H. Scott-Gagan, B. Parker, D. Griffin, M. Nongkas, M.T. McCulloch. 2004. Geochemistry of coral from Papua New Guinea as a proxy for ENSO ocean-atmospheric interactions in the Pacific Warm Pool. *Continental Shelf Research* 24: 2343-2356.
- Barnes, D.J. and J.M. Lough. 1993. On the nature and causes of density banding in massive coral skeletons. *Journal of Marine Biology and Ecology* 167: 91-108.
- Beck, J.W., R.L. Edwards, E. Ito, F.W. Taylor, J. Recy, F. Rougerie, P. Joannot, and C. Henin. 1992. Sea-surface temperature from coral skeletal strontium/calcium ratios. *Science, New Series* 257 (5070): 644-647.
- Bell, T., J.W. Jenson, M.A. Lander, R.H. Randall, J.W. Partin, B. Hardt, and J.L. Banner. 2011. Coral and speleothem *in situ* monitoring and geochemical analysis: Guam, Mariana Islands, USA. University of Guam Water and Environmental Research Institute Technical Report No. 136.
- Bell, T., T. Endo, W. Jenson, R.F. Bell, and M.A. Lander. 2011. Pneumatic underwater drill for extracting coral cores. University of Guam Water and Environmental Research Institute Technical Report No. 135.
- Burdick, D., V. Brown, J. Asher, C. Caballes, M. Gawel, L. Goldman, A. Hall, J. Kenyon, T. Leberer, E. Lundblad, J. McIlwain, J. Miller, D. Minton, M. Nadon, N. Pioppi, L. Raymundo, B. Richards, R. Schroeder, P. Schupp, E. Smith, and B.

- Zgliczynski. 2008. Status of the Coral Reef Ecosystems of Guam. Bureau of Statistics and Plans, Guam Coastal Management Program. iv + 76 pp.
- Caldow, C. and G.M. Wellington. 2003. Patterns of annual increment formation in otoliths of pomacentrids in the tropical western Atlantic: implications for population age-structure examination. *Marine Ecology Progress Series* 265: 185-195.
- Charles, C.D., D.E. Hunter, R.G. Fairbanks. 1997. Interaction between the ENSO and the Asian Monsoon in a coral record of tropical climate. *Science* 277: 924-928.
- Chowdhury, M.R., P.S. Chu, and T. Schroeder. 2007. ENSO and seasonal sea-level variability—A diagnostic discussion for the U.S.-Affiliated Pacific Islands. *Theoretical and Applied Climatology* 88: 213-234.
- Cleveland, R.O., A.L. Cohen, R.A. Roy, H. Singh, and T. Szabo. Imaging coral II: using ultrasound to image coral skeleton. *Subsurface Sensing Technologies and Applications* 5(1): 43-61.
- Cobb, K.M., C.D. Charles, H. Cheng, and R.L. Edwards. 2003. El Nino/Southern Oscillation and tropical Pacific climate during the last millennium. *Nature* 424: 271-276.
- Cohen, A., K.E. Owens, G.D. Layne, and N. Shimizu. 2002. The effect of algal symbionts on the accuracy of Sr/Ca paleotemperatures from coral. *Science* 296: 331-333.
- Cohen, A., G.D. Layne, and S.R. Hart. 2001. Kinetic control of skeletal Sr/Ca in a symbiotic coral: implications for the paleotemperature proxy. *Paleoceanography* 16(1): 20-26.
- Cohen, A. and T. McConnaughey. 2003. Geochemical perspectives on coral mineralization. *Reviews in Mineral Geochemistry* 54:151-187.
- Cohen, A. and S.R. Hart. 2004. Deglacial sea surface temperatures of the western tropical Pacific: a new look at old coral. *Paleoceanography* 19: PA4031.
- Cohen, A. and R.A. Sohn. 2004. Tidal modulation of Sr/Ca ratios in a Pacific reef coral. *Geophysical Research Letters* 31: L16310.
- Correge, T. 2006. Sea surface temperature and salinity reconstruction from coral geochemical tracers. *Palaeogeography, Palaeoclimatology, Palaeoecology* 232: 408-428.

- Cravatte, S., T. Delcroix, D. Zhang, M. McPhaden, and J. Leloup. 2009. Observed freshening and warming of the Western Pacific Warm Pool. *Climate Dynamics* 33: 565-589.
- Crook, E. D., A. L. Cohen, M. Rebolledo-Vieyra, L. Hernandez, and A. Paytan. 2013. Reduced calcification and lack of acclimatization by coral colonies growing in areas of persistent natural acidification. *Proceedings of the National Academy of Sciences*.
- Deng, W., G. Wei, L. Xie, T. Ke, Z. Wang, T. Zeng, and Y. Lui. 2013. Variations in the Pacific Decadal Oscillation since 1853 in a coral record from the northern South China Sea. *Journal of Geophysical Research-Oceans* 118: 1-9.
- deVilliers, S. 1999. Seawater strontium and Sr/Ca variability in the Atlantic and Pacific oceans. *Earth and Planetary Science Letters* 171: 623-634.
- Fairbanks, R.G., M.N. Evans, J.L. Rubenstone, R.A. Mortlock, K. Broad, M.D. Moore, and C.D. Charles. 1997. Evaluating climate indices and their geochemical proxies measured in corals. *Coral Reefs* 16:S93-S100.
- Fallon S., M. McCulloch, and M. Shelley. 2001. Measuring elemental ratios in corals by LA-ICP-MS. Agilent Technologies, Inc. 5988-3742EN
- Ferrier-Pages, C., F. Boisson, D. Allemand, and E. Tambutte. 2002. Kinetics of strontium uptake in the scleractinian coral *Stylophora pistillata*. *Marine Ecology Progress Series* 245: 93-100.
- Gagan, M.K., L.K. Ayliffe, D. Hopley, J.A. Cali, G.E. Mortimer, J. Chappell, M.T. McCulloch, and M.J. Head. 1998. Temperature and surface-ocean water balance of the mid-Holocene tropical western. *Pacific Science* 279: 1014-1018.
- Gagan, M.K., L.K. Ayliffe, J.W. Beck, J.E. Cole, E.R.M. Druffel, R.B. Dunbar, D.P. Schrag. 2000. New views of tropical paleoclimates from corals. *Quaternary Science Reviews* 19: 45-64.
- Goodkin, N.F., K.A. Hughen, A.L. Cohen, and S.R. Smith. 2005. Record of Little ice age sea surface temperatures at Bermuda using growth-dependent calibration of Sr/Ca. *Paleoceanography* 20: PA4016.
- Goodkin, N.F., K.A. Hughen, and A.L. Cohen. 2007. A multicoral calibration method to approximate a universal equation relating Sr/Ca and growth rate to sea surface temperature. *Paleoceanography* 22: PA1214.
- Guilderson, T.P. and D.P. Schrag. 1998. Abrupt shifts in subsurface temperatures in the tropical Pacific associated with changes in El Niño. *Science* 281: 240-243.

- Houck, J.E., R.W. Buddemeier, S.V. Smith, and P.L. Jokiel. 1977. The response of coral growth rate and skeletal strontium content to light intensity and water temperature. *Proceedings of the Third International Coral Reef Symposium* 425-432.
- Lander, M.A. and C.P. Guard. 2003. Creation of a 50-Year rainfall database, annual rainfall climatology, and annual rainfall distribution map for Guam. University of Guam Water and Environmental Research Institute Technical Report 102.
- Lough, J.M. and D.J. Barnes. 1990. Intra-annual timing of density band formation of Porites coral from the central Great Barrier Reef. *Journal of Experimental Marine Biology and Ecology* 135(1): 35-57.
- Lough, J.M. and D.J. Barnes. 1997. Several centuries of variation in skeletal extension, density and calcification in massive *Porites* colonies from the Great Barrier Reef: a proxy for seawater temperature and a background of variability against which to identify unnatural change. *Journal of Experimental Marine Biology and Ecology* 211: 29-67.
- Lough, J.M. and D.J. Barnes. 2000. Environmental controls on growth of the massive coral Porites. *Journal of Experimental Marine Biology and Ecology* 245: 225-243.
- Lough, J.M., D.J. Barnes, and R.B. Taylor. 1997. Understanding growth mechanisms: the key to successful extraction of proxy climate records from corals. *Proceedings of the Eight International Coral Reef Symposium 2*: 1697-1700.
- Liu, J., T. J. Crowley, T. M. Quinn, and F. W. Taylor. 2012. Assessment of SST-Sr/Ca Decoupling in Western Pacific Warm Pool corals. Manuscript submitted for publication.
- Maupin, C. R. 2008. Extracting a climate signal from the skeletal geochemistry of the caribbean coral *Siderastrea siderea*. *University of South Florida Theses and Dissertations* Paper 384.
- McCulloch, M.T., M.K. Gagan, G.E. Mortimer, A.R. Chivas, and P.J. Isdale. 1994. A high-resolution Sr/Ca and delta18O coral record from the Great Barrier Reef, Australia, and the 1982-1983 El Nino. *Geochimica et Cosmochimica Acta* 58(12): 2747-2754.
- Meekan, M.G., G.M. Wellington, L. Axe. 1999. El Nino-Southern Oscillation events produce checks in the otoliths of coral reef fishes in the Galapagos Archipelago. *Bulletin of Marine Science* 64(2): 383-390.

- Merrifield, M.A. 2011. A shift in Pacific sea level trends. *Journal of Climate* 24: 4126-4138.
- Min, G.R., R.L. Edwards, F.W. Taylor, J. Recy, C.D. Gallup, and J.W. Beck. 1995. Annual cycles of U/Ca in coral skeletons and U/Ca thermometry. *Geochimica et Cosmochimica Acta* 59(10): 2025-2042.
- Muller-Parker, G. and C. F. D'Elia. 1997. Interactions between corals and their symbiotic algae. Pp. 96–133 in C. Birkeland, ed. *Life and death of coral reefs*. Chapman & Hall, New York.
- Ourbak, T., T. Correge, B. Malaize, F. Le Cornec, K. Charlier, and J.P. Peypouquet. 2006. ENSO and inter-decadal variability over the last century document by geochemical records of two coral cores from the South West Pacific. *Advances in Geosciences* 6: 23-27.
- Parmesan, C. 2006. Ecological and Evolutionary Responses to Recent Climate Change. *Annual Reviews in Ecological and Evolutionary Systems* 37: 637-669.
- Prouty, N. 2013. Reconstruction of climate change and land-use history from Guam as derived from coral geochemical records spanning the last 1-2 centuries. Manuscript in preparation.
- Purdey, M. 2004. Elevated levels of ferrimagnetic metals in foodchains supporting the Guam cluster of neurodegeneration: Do metal nucleated crystal contaminants evoke magnetic fields the initiate the progressive pathogenesis of neurodegenerations? *Medical Hypotheses* 63: 793-809.
- Quinn, T.M. and D.E. Sampson. 2002. A multiproxy approach to reconstructing sea surface conditions using coral skeleton geochemistry. *Marine Science Faculty Publications* Paper 111.
- Ramos, A.A., Y. Inoue, and S. Ohde. 2004. Metal contents in *Porites* corals: anthropogenic input of river run-off into a coral reef from an urbanized area, Okinawa. *Marine Pollution Bulletin* 24: 281-294.
- Reynaud, S., C. Ferrier-Pages, F. Boisson, D. Allemand, and R.G. Fairbanks. 2004. Effect of light and temperature on calcification and strontium uptake in the scleractinian coral *Acropora verweyi*. *Marine Ecology Progress Series* 279: 105-112.
- Rosenfeld, M., A. Shemesh, R. Yam, K. Sakai, and Y. Loya. Impact of the 1998 bleaching event on δO^{18} records of Okinawa corals. *Marine Ecology Progress Series* 314: 127-133.

- Sea Engineering, Inc. 2010. Physical oceanographic monitoring of dredging and construction activities at Kilo Wharf: September 2008- December 2009. Final Report.
- Secor, D.H., J.R. Rooker, E. Zlokovitz, and V.S. Zdanowicz. 2001. Identification of riverine, estuarine, and coastal contingents of Hudson River striped bass based upon otolith elemental fingerprints. *Marine Ecology Progress Series* 211: 245-253.
- Smith, S.V., R.W. Buddemeier, R.C. Redalje, and J.E. Houck. 1979. Strontium-calcium thermometry in coral skeletons. *Science, New Series* 204: 404-407.
- Stephans, C.L., T.M. Quinn, F.W. Taylor, and T. Correge. 2004. Assessing the reproducibility of coral-based climate records. *Geophysical Research Letters* 31: L18210.
- Storlazzi, C., M.K. Presto, and J.B. Logan. 2009. Coastal circulation and sediment dynamics in War-in-the-Pacific National Historical Park. USGS Open File-Report 2009-1195.
- Storlazzi, C., O.M. Cheriton, J.M.R. Lescinski, and J.B. Logan. 2013. Coastal circulation and water-column properties in War in the Pacific National Historical Park, Guam. USGS report in progress.
- Stojkovich, J.O. 1977. Survey and species inventory of representative pristine marine communities on Guam. University of Guam Marine Lab Tech Report 40.
- Sun, Y., M. Sun, T. Lee, and B. Nie. 2005. The influence of seawater Sr content on Sr/Ca and Sr thermometry. *Coral Reefs* 24: 23-29.
- Swart, P.K., H. Elderfield, and M.J. Greaves. 2002. A high-resolution calibration of Sr/Ca thermometry using the Caribbean coral *Montastraea annularis*. *Geochemistry, Geophysics, and Geosystems* 3(11): 1525-2027.
- Turekian, K.K. 1996. Global Environmental Change: Past, Present, and Future. Prentice Hall pp. 200.
- Wang, C., C. Deser, J.Y. Yu, P. DiNezio and A. Clement. 2012. El Niño Southern Oscillation (ENSO): A Review. In P. Glymn, D. Manzello and I. Enochs, eds, Coral Reefs of the Eastern Pacific. Spring Science Publisher.
- Weber, J.N. 1973. Incorporation of strontium into reef coral skeletal carbonate. *Geochimica et Cosmochimica Acta* 37: 2173-2190.
- Weber, J.N., E.W. White, and P.H. Weber. 1975. Correlation of density banding in reef coral skeletons with environmental parameters: the basis for interpretation of

chronological records preserves in the coralla of corals. *Paleobiology* 1(2): 137-149.

Wei, G., M. Sun, X. Li, and B. Nie. 2000. Mg/Ca, Sr/Ca, and U/Ca ratios of a *Porites* coral from Sanya Bay, Hainan Island, South China Sea and their relationship to sea surface temperature. *Palaeogeography, Palaeoclimatology, and Palaeoecology* 162: 59-74.

Appendix A: Coral core metadata and colony photographs

Table A-1 Coral colony coordinates and diver information

Colony ID	Dive Time(ChST)	Lat(WGS84)	Lon(WGS84)	Divers
Agat1	4/26/2012 12:17	13.3582813	144.6426375	Amanda deVillers, John Jenson, Josh Logan, Nancy Prouty, Curt Storlazzi
Agat2	4/26/2012 15:04	13.3579446	144.6427629	Amanda deVillers, John Jenson, Josh Logan, Nancy Prouty, Curt Storlazzi
Apra1	4/27/2012 8:48	13.4624604	144.647775	Josh Logan, Nancy Prouty, Curt Storlazzi
Apra2	4/27/2012 8:34	13.4638809	144.6450969	Josh Logan, Nancy Prouty, Curt Storlazzi
Asan1	4/28/2012 12:14	13.4765641	144.7158928	Amanda deVillers, Josh Logan, Nancy Prouty, Curt Storlazzi
Asan2	4/28/2012 15:28	13.4775356	144.7123592	Josh Logan, Nancy Prouty, Curt Storlazzi

Table A-2 Coral colony dimensions. Width and height measurements were estimated using a transect tape while free diving (due to SCUBA diving restrictions).

These describe the widest and tallest parts of the colony.

Colony ID	Depth (m)	Width (m)	Height (m)
Agat1	5.5	3.7	2.4
Agat2	5.5	3.7	2.4
Apra1	2.4	1.4	0.8
Apra2	1.2	1.2	0.6
Asan1	10.1	1.5	2.1
Asan2	7.6	1.2	0.8



Figure A-1 Whole colony view of Agat1 in April 2012, prior to coring.



Figure A-2 Whole colony view of Agatlin April 2012, during coring.



Figure A-3 Whole colony view of Agat1 in March 2013, one year after coring.

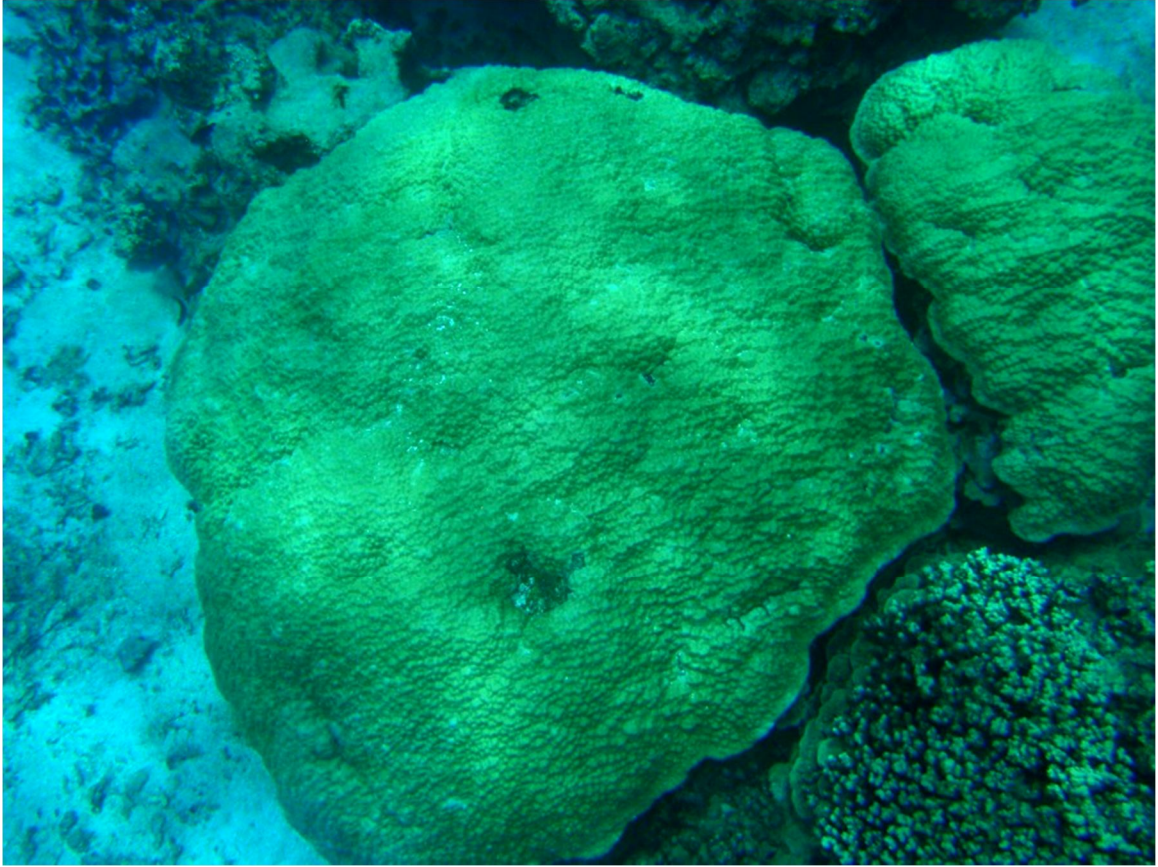


Figure A-4 Whole colony view of Agat2 in April 2012, prior to coring.



Figure A-5 Whole colony view of Agat2 in March 2012, one year after coring.



Figure A-6 Whole colony view of Asan1 April 2012, prior to coring.



Figure A-7 Whole colony view of Asan2 April 2012, during coring.



Figure A-8 Whole colony view of Apra1 in April 2012, prior to coring.



Figure A-9 Whole colony view of Apra1in November 2012, after coring.

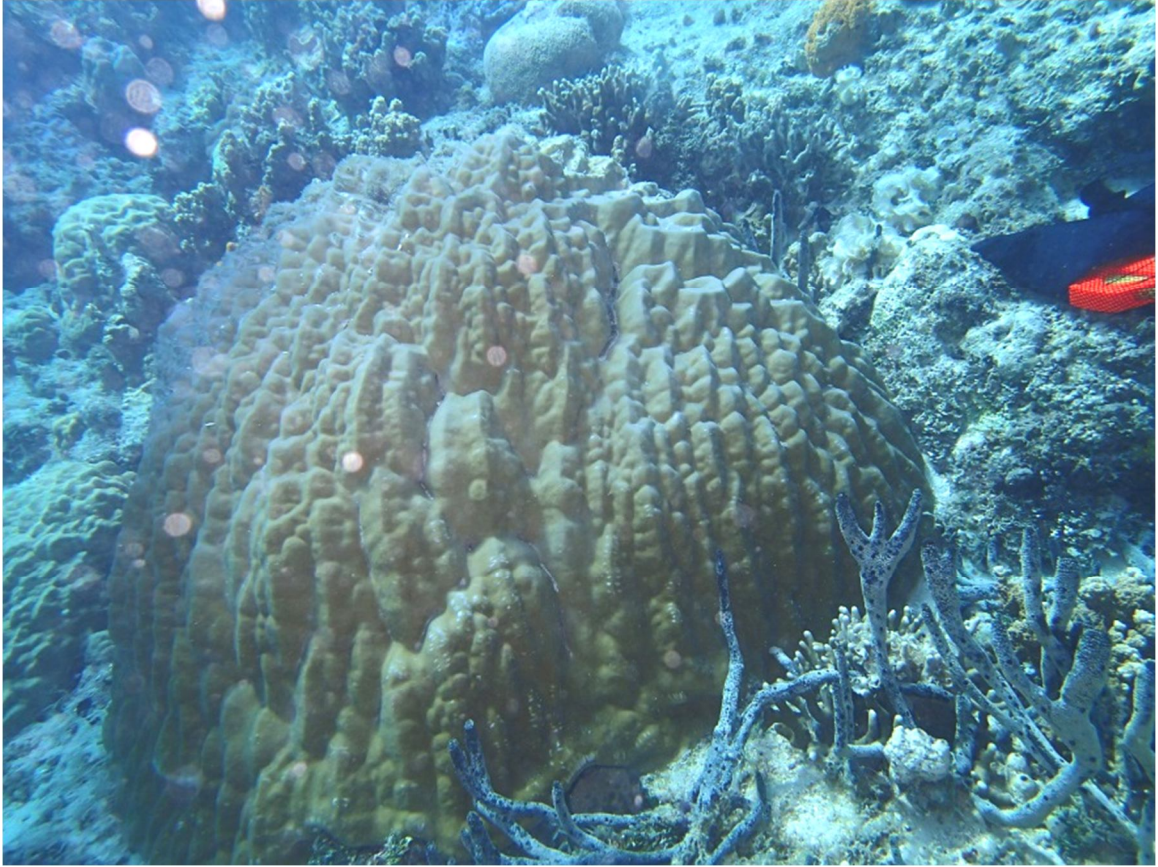


Figure A-10 Whole colony view of Apra2 in November 2012, after coring.

Appendix B: Sea surface temperature (SST) dataset comparison

Sea surface temperature (SST) from the Asan and Agat reef flats were compared against the oceanic measurements of SST in the area. Hobo pendant temperature loggers (Onset Corp ®) were placed at in Asan and in Agat just inside the reef crest at both locations. The loggers recorded hourly temperature measurements on the hour from September 28, 2012 to December 17, 2012. Hourly SST data were downloaded from the CDIP wave buoy off Ipan, Guam via <http://cdip.ucsd.edu/>. SST data were also downloaded from the Hadley (<http://coastwatch.pfeg.noaa.gov/erddap/griddap/erdHadISST.html>), but are only available at monthly resolution, so they were not directly comparable to the reef flat logger data sets.

The reef flat loggers showed similar SST trends, although the temperature in Asan tended to be warmer during the day than in Agat. Both loggers showed an increase in range of temperatures beginning in mid-October. Not surprisingly, the range in temperature experienced at the Ipan buoy was drastically less than on the reef flat sites. Average daily temperatures were similar between the buoy and the logger sites, although in some cases when average temperatures increased, there was a one to two day lag between the buoy and the logger sites (Fig B-1, Table B-1).

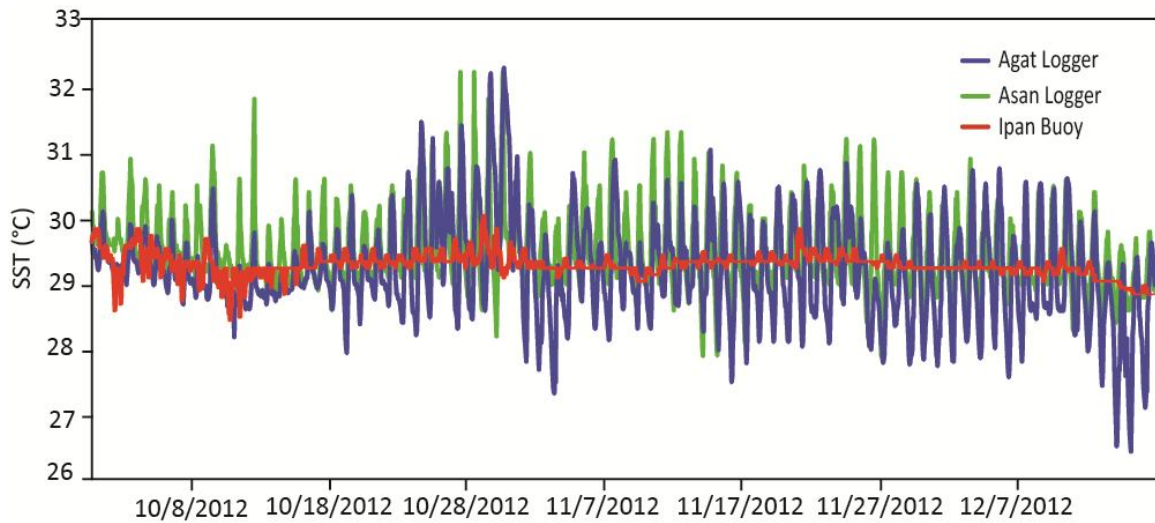


Figure B-1 SST from reef flat HOBO loggers in Asan and Agat compared with SST from the CDIP Wave Buoy in off of Ipan from September 28, 2012 to December 17, 2012. All three datasets are hourly measurements, taken on the hour.

Table B-1 Descriptive statistics for the Asan and Agat reef flat HOBO loggers and the CDIP Wave Buoy off of Ipan for hourly measurements taken between September 28, 2012 and December 17, 2012.

	Agat Logger	Asan Logger	Ipan Buoy
Average	29.16	29.44	29.24
Max	32.25	32.19	30.00
Min	26.40	27.86	28.40
SD	0.77	0.58	0.18

Monthly averages of the hourly Ipan buoy SST data were compared with the Hadley SST dataset (Fig B-2). These datasets are very similar, correlating with an R^2 of 0.970 ($p < 0.0001$).

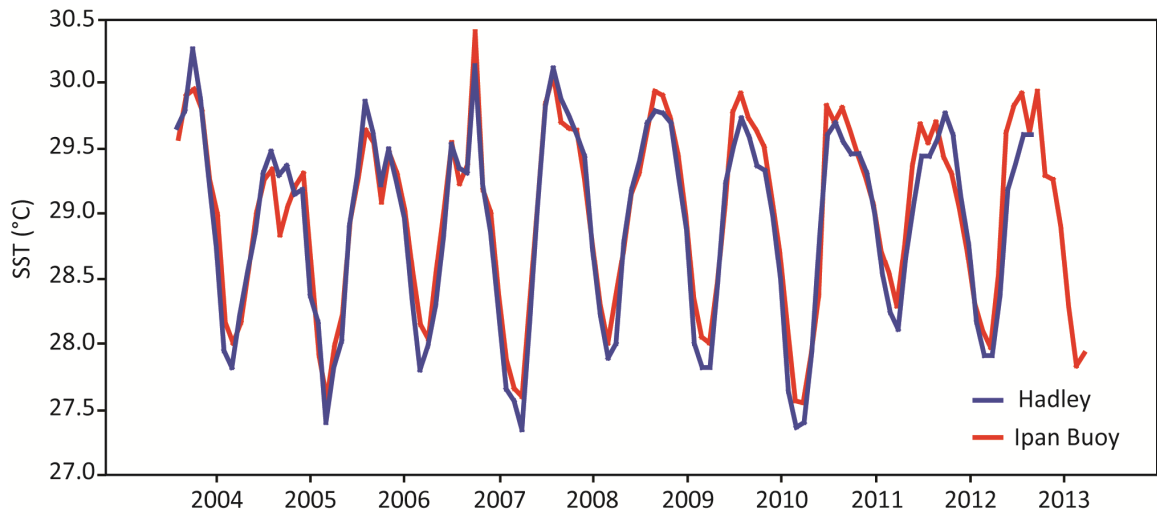


Figure B-2 SST data from Hadley 13-14 degrees N, 144-145 degrees E compared with SST from the CDIP wave buoy off of Ipan, Guam for the time period July 2003 to March 2013. Both datasets are averaged to monthly values.

Appendix C: Raw Sr/Ca datasets

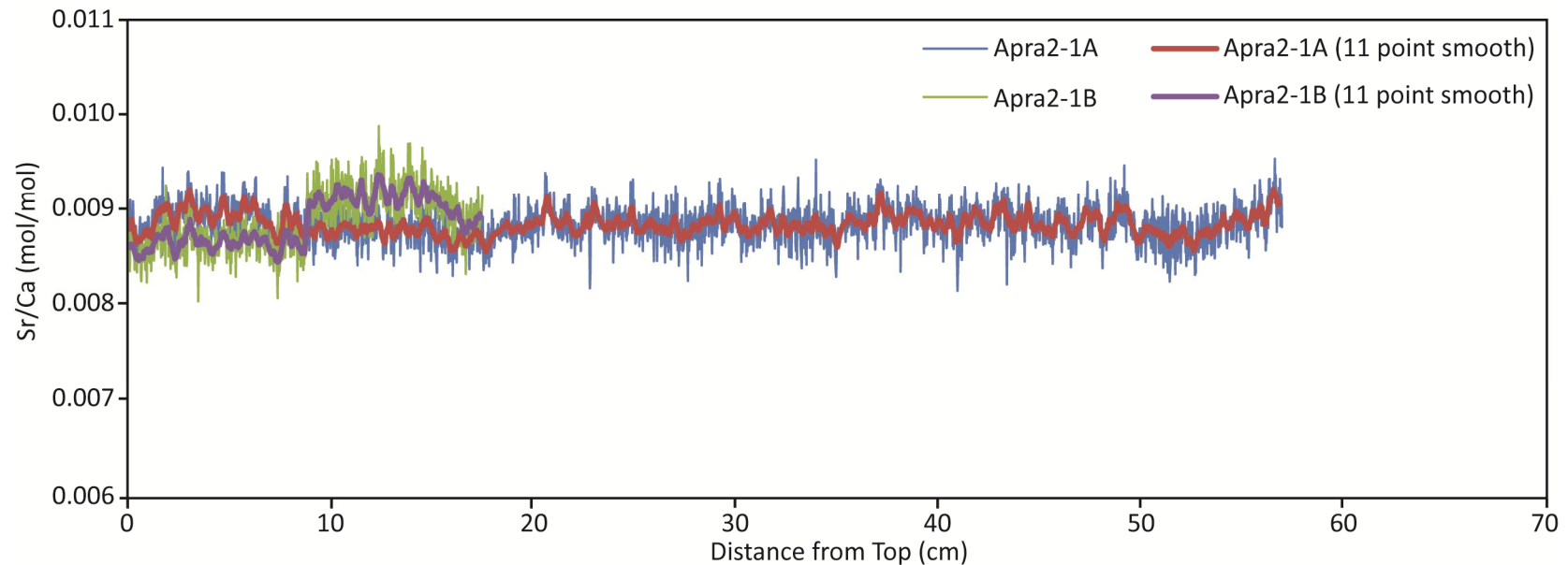


Figure C-1 Raw Sr/Ca values from Apra2-1 as measured at distances from the top of the core (most recent skeletal material) to the bottom (oldest skeletal material). A and B indicate two separate transects along which Sr/Ca was measured as replicates. The thicker lines indicate the 11-point moving average of the raw data set.

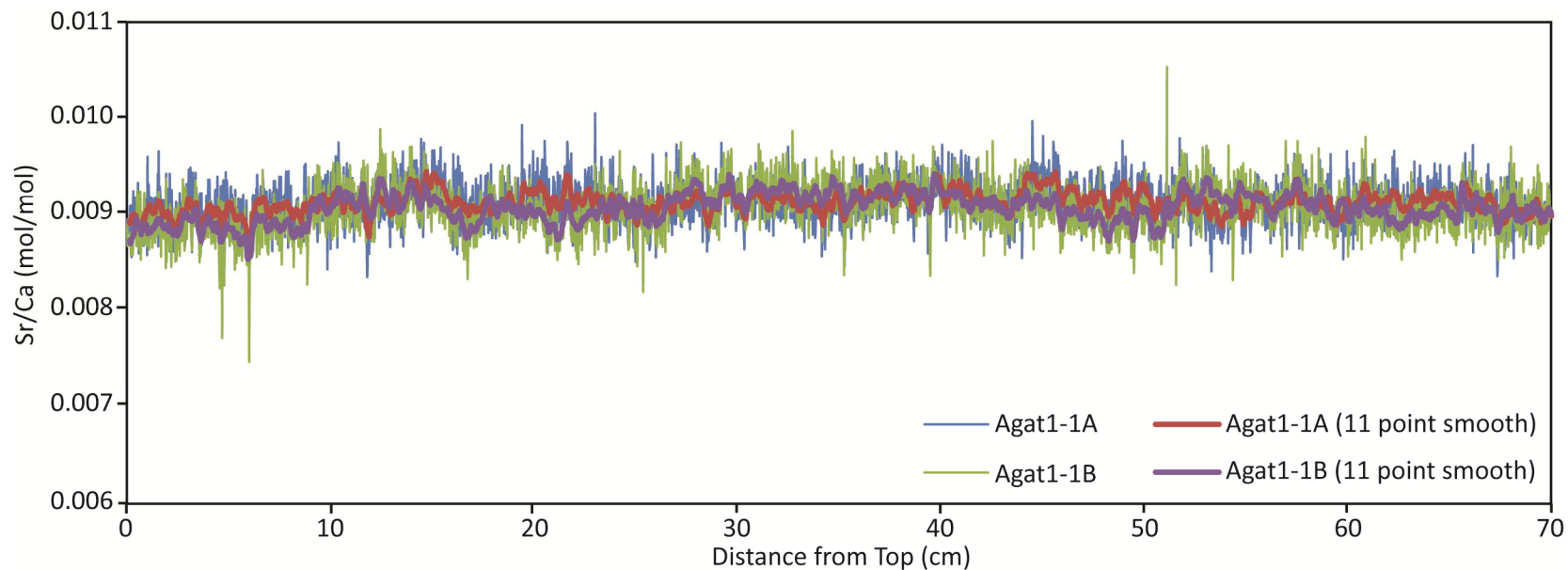


Figure C-2 Raw Sr/Ca values from Agat1-1 for the first 70 cm of each transect as measured at distances from the top of the core (most recent skeletal material) to the bottom (oldest skeletal material). A and B indicate two separate transects along which Sr/Ca was measured as replicates. The thicker lines indicate the 11-point moving average of the raw data set.

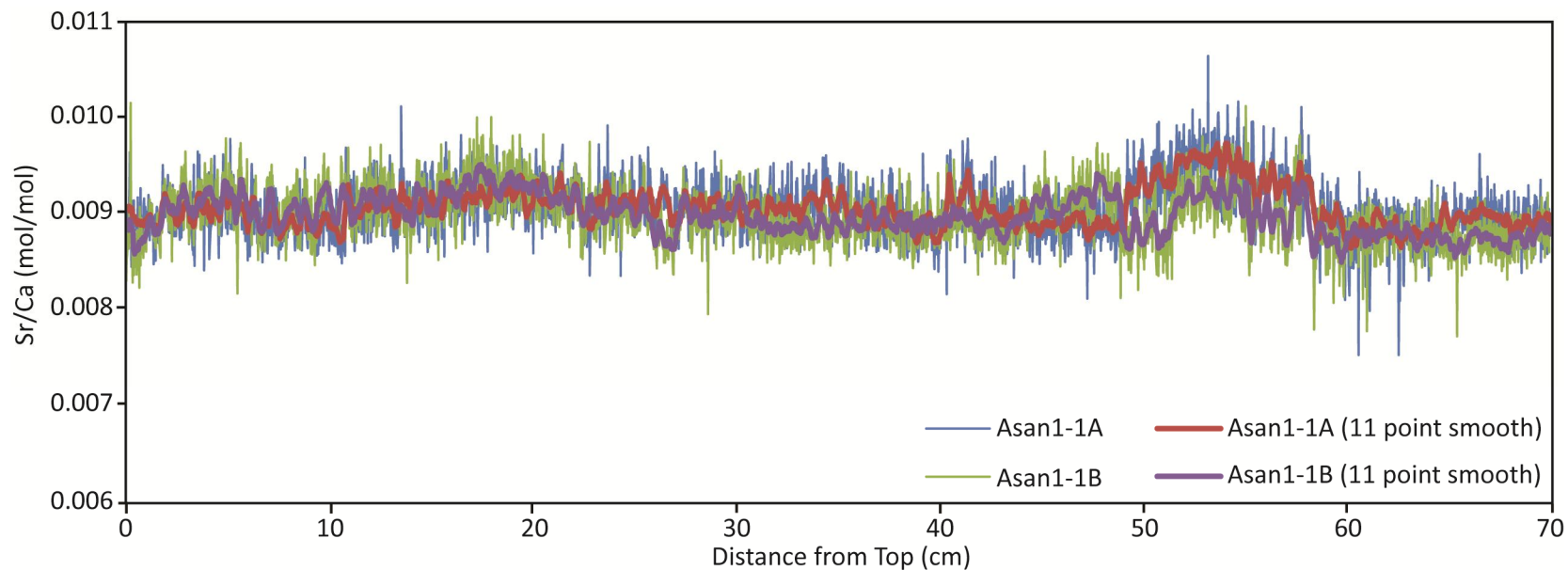


Figure C-3 Raw Sr/Ca values from Asan1-1 for the first 70 cm of each transect as measured at distances from the top of the core (most recent skeletal material) to the bottom (oldest skeletal material). A and B indicate two separate transects along which Sr/Ca was measured as replicates. The thicker lines indicate the 11-point moving average of the raw data set.

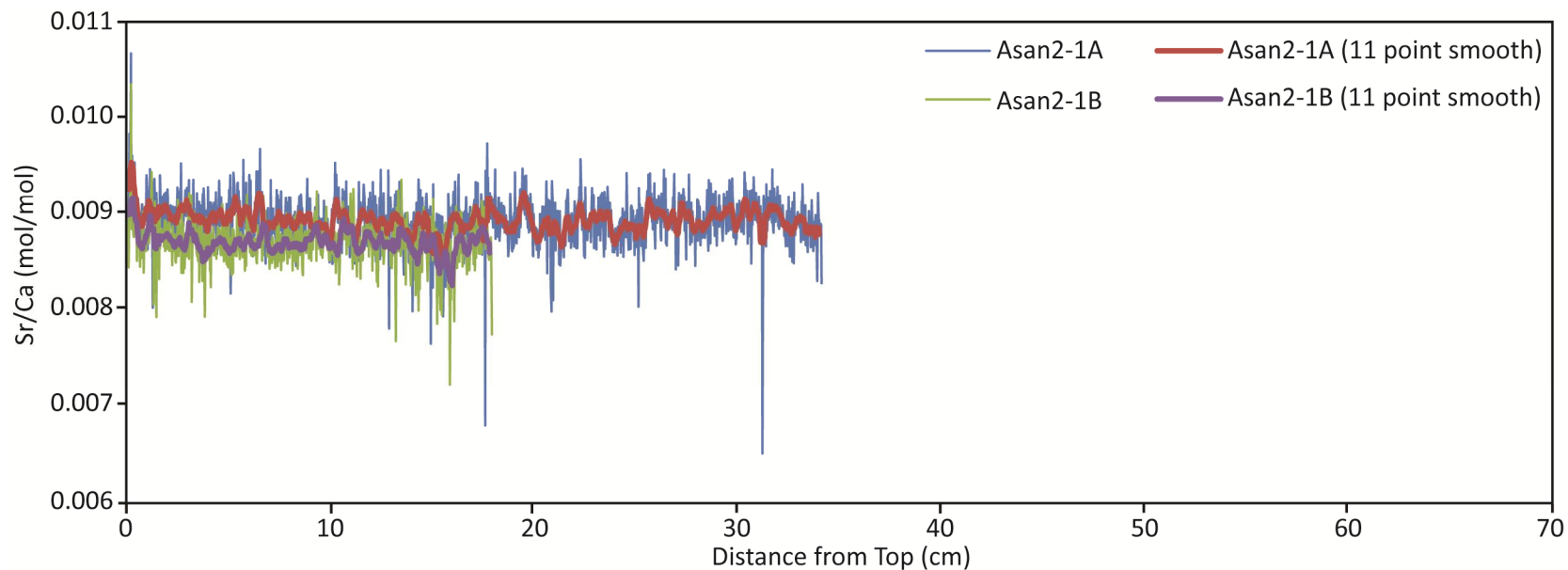


Figure C-4 Raw Sr/Ca values from Asan2-1 as measured at distances from the top of the core (most recent skeletal material) to the bottom (oldest skeletal material). A and B indicate two separate transects along which Sr/Ca was measured as replicates. The thicker lines indicate the 11-point moving average of the raw data set.

Appendix D Empirical Orthogonal Function (EOF) Analysis

Table D-1 Percent of total variance explained by each EOF mode. EOF analysis was performed on 1985-2010 monthly Sr/Ca data for each site.

Core	EOF1	EOF2	EOF3	EOF4	EOF5
Agat1-1	44.1	27.5	14.0	10.0	4.5
Apra2-1	40.6	27.5	15.2	9.1	7.6
Asan1-1	49.2	21.1	16.9	9.8	3.0
Asan2-1	39.5	23.1	20.0	9.8	7.6

Table D-2 Normalized Eigenmodes for each EOF mode and each metal/Ca ratio.

Core	Metal/Ca	EOF1	EOF2	EOF3	EOF4	EOF5
Agat1-1	B/Ca	0.005	0.828	-0.496	-0.252	0.068
	Ba/Ca	-0.066	0.785	0.610	0.088	0.018
	Mg/Ca	-0.782	0.150	-0.242	0.551	0.057
	Sr/Ca	0.914	-0.029	-0.023	0.210	0.345
	U/Ca	0.868	0.221	-0.144	0.284	-0.311
Apra2-1	B/Ca	-0.645	0.157	0.723	-0.151	0.123
	Ba/Ca	-0.359	0.823	-0.183	-0.221	-0.334
	Mg/Ca	-0.743	0.387	-0.318	0.272	0.352
	Sr/Ca	0.746	0.452	-0.041	-0.333	0.356
	U/Ca	0.614	0.565	0.317	0.445	-0.073
Asan1-1	B/Ca	-0.492	-0.469	0.690	0.249	-0.025
	Ba/Ca	-0.102	0.879	0.464	-0.029	-0.036
	Mg/Ca	-0.790	0.242	-0.306	0.444	0.163
	Sr/Ca	0.854	0.077	-0.083	0.472	-0.187
	U/Ca	0.924	-0.017	0.233	0.072	0.295
Asan2-1	B/Ca	-0.232	0.181	0.941	-0.147	0.073
	Ba/Ca	0.152	0.905	-0.214	-0.320	-0.098
	Mg/Ca	-0.706	0.486	0.002	0.514	-0.039
	Sr/Ca	0.835	0.258	0.045	0.223	0.429
	U/Ca	0.838	0.039	0.257	0.228	-0.422

Table D-3 Percent of variance of each metal/Ca ratio explained by each EOF mode.

Core	Metal/Ca	EOF1	EOF2	EOF3	EOF4	EOF5
Agat1-1	B/Ca	0.003	68.545	24.630	6.360	0.462
	Ba/Ca	0.440	61.575	37.171	0.782	0.032
	Mg/Ca	61.215	2.261	5.859	30.341	0.323
	Sr/Ca	83.570	0.085	0.055	4.412	11.878
	U/Ca	75.335	4.893	2.070	8.043	9.660
Apra2-1	B/Ca	41.543	2.477	53.203	2.274	1.503
	Ba/Ca	12.915	67.652	3.359	4.899	11.175
	Mg/Ca	55.166	14.949	10.125	7.372	12.387
	Sr/Ca	55.610	20.466	0.172	11.107	12.645
	U/Ca	37.705	31.906	10.020	19.835	0.534
Asan1-1	B/Ca	24.160	22.036	47.549	6.191	0.064
	Ba/Ca	1.035	77.177	21.572	0.084	0.132
	Mg/Ca	62.428	5.845	9.368	19.697	2.663
	Sr/Ca	72.913	0.588	0.686	22.299	3.514
	U/Ca	85.297	0.029	5.423	0.523	8.727
Asan2-1	B/Ca	5.404	3.288	88.625	2.151	0.532
	Ba/Ca	2.299	81.956	4.562	10.225	0.957
	Mg/Ca	49.823	23.641	0.001	26.385	0.151
	Sr/Ca	69.796	6.656	0.200	4.964	18.384
	U/Ca	70.213	0.151	6.619	5.186	17.831